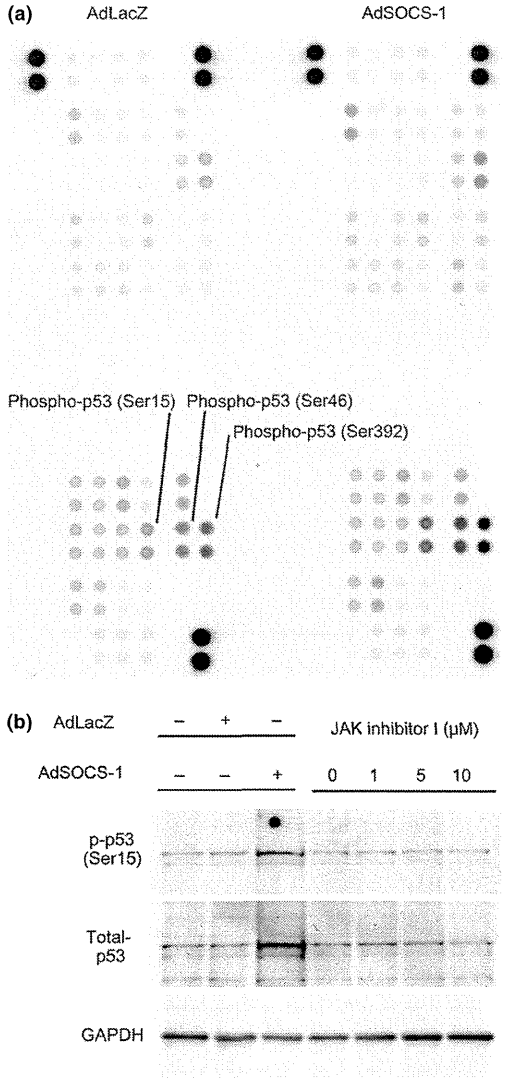

Fig. 5. Protein p53 is upregulated by adenovirus vector containing suppressor of cytokine signaling-1 (AdSOCS-1) in A549 lung cancer cells. (a) A549 cells were cultured in RPMI-1640 medium containing 10% FBS with AdSOCS-1 at an MOI of 40. After a 24-h culture, protein extracts were examined with a phospho-kinase array with each phosphorylated protein identified in duplicate. The double-labeled spots in the upper right corner represent the positive controls. (b) Cell lysates were prepared 48 h after infection with AdLacZ or AdSOCS-1 at an MOI of 40. Cell lysates were immunoblotted with anti-phospho-53 (p-p53 [Ser15]) and anti-p53 antibodies. (c) Cell lysates were prepared 48 h after exposure to 5 μM JAK inhibitor I and immunoblotted with anti-p-p53 (Ser15) and anti-p53 antibodies.

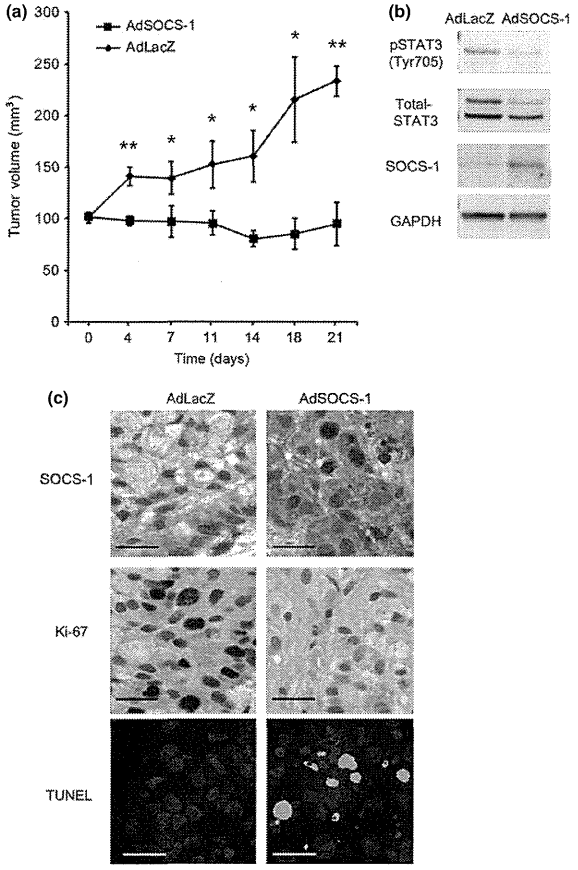

Fig. 6. Suppressor of cytokine signaling-1 (SOCS-1) shows antitumor activity in a lung cancer xenograft model. (a) Female ICR nu/nu mice were s.c. implanted with 2×10^6 A549 cells in their flank. When the calculated tumor volumes reached to approximately 100 mm^3, 4×10^8 pfu AdSOCS1 or AdLacZ adenoviral vectors were intratumorally treated twice per week. Tumor volumes were determined twice per week. The mean volume ± SEM of five tumors in each group, and were analyzed by Student's *t*-test (**P* < 0.05, ***P* < 0.01). (b) Western blot analysis of phosphorylated signal transducer and activator of transcription 3 (pSTAT3), STAT3, SOCS-1, and GAPDH in A549 tissues from AdSOCS-1 or AdLacZ injected animals. Lysates from tumors were analyzed by Western blotting. (c) Immunohistochemical analysis of SOCS-1, Ki-67, and TUNEL (blue fluorescence, DAPI staining for nuclei; cyan fluorescence, TUNEL positivity) in A549 tissues from animals injected with AdSOCS-1 or AdLacZ. Scale bar = 25 μm.

(4×10^8 pfu) intratumorally twice per week significantly suppressed tumor growth compared to control AdLacZ injection (Fig. 6a). AdSOCS-1 *in vivo* could modulate intracellular signaling in NSCLC cells as *in vitro*, as Western blot analysis showed that phosphorylation levels of STAT3 were decreased in the A549 tissues from AdSOCS-1 injected animals (Fig. 6b). Furthermore, few Ki-67-positive nuclei were detected by immunohistochemical analysis in AdSOCS-1 infected tissues compared to AdLacZ, indicating that proliferating cells are decreased by overexpression of SOCS-1 (Fig. 6c). Additionally, induction of apoptosis was detected in AdSOCS-1 infected A549 tissue compared to AdLacZ by TUNEL analysis (Fig. 6c).

Discussion

In this study, we investigated the possibility that SOCS-1 could be used in LC therapies. Previous reports showed that PC9 harbors a deletion mutation in EGFR and that A549 and LU65 cells possess wild-type EGFR.[34,39] Although EGFR mutation in NSCLC was previously reported to activate AKT, MAPK, and STAT3 signaling,[40] our research showed that STAT3 was more strongly expressed in A549 and LU65 than in PC9 cells, and that sensitivity to overexpression of SOCS-1 was also higher in A549 and LU65 cells than in PC9 (Fig. 1). In addition, JAK inhibitor I significantly suppressed proliferation of A549 and LU65 cells, but not of PC9. Therefore, we consider that the marked antiproliferative effect by overexpression of SOCS-1 on A549 and LU65 cells, but not on PC9, was

attributable to the inhibition of JAK/STAT3 pathway *in vitro*. As SOCS-1 also shows an antiproliferative effect *in vivo* (Fig. 6), AdSOCS1 gene therapy might be effective for patients with NSCLC, in which the JAK/STAT3 signaling pathway is constitutively activated. It has been reported that approximately 50% of NSCLC tumors showed elevated phosphorylation levels of STAT3 (Tyr705) by immunohistochemical analysis.[4] There is a further possibility that LC patients harboring STAT3 dependence, detected by immunostaining analysis of phosphorylation levels of STAT3 (Tyr705) in specimens obtained surgically or bronchoscopically, could be selected for treatment with SOCS-1 overexpression.

Comparative analyses of the antiproliferative effects of *SOCS-1* gene introduction and JAK inhibitor I treatment suggest that overexpression of SOCS-1 may have a stronger effect than that of the JAK inhibitor I on A549 and LU65 cells (Fig. 2e). In fact, SOCS-1, but not JAK inhibitor I, inhibited FAK and EGFR, which are important for the survival of A549 cells. In addition, the combined effect of FAK siRNA and JAK inhibitor I, or that of PD153035 and JAK inhibitor I, was superior to the antiproliferative effect of JAK inhibitor alone (Figs 3,4). These findings suggest that the potent antiproliferative effect of SOCS-1 depends not only on JAK inhibition but also on the suppression of other distinct signal transduction pathways, such as FAK and EGFR. In addition, phosphorylation of p53 at Ser15 was enhanced by the overexpression of the *SOCS-1* gene in A549 cells (Fig. 5). Because phosphorylation of p53 at Ser15 contributes to antitumor effects under certain experimental conditions,[35–38] and A549 cells express wild-type p53,[41] activation of p53 by SOCS-1 overexpression seems to be involved in the antitumor effects.[42]

In conclusion, the findings of our study suggest that *SOCS-1* gene therapy is potentially effective for at least a subset of NSCLC both *in vitro* and *in vivo*. It was shown that SOCS-1 had a potent antiproliferative effect on JAK-dependent NSCLC cells by targeting the JAK/STAT3 pathway. In addition, SOCS-1 successfully targeted many factors such as FAK, EGFR, and p53 in NSCLC cells. It is thus possible that *SOCS-1* gene therapy could have a unique advantage over JAK inhibitor for the treatment of NSCLC.

Further studies will be needed to elucidate the mechanism of JAK/STAT3 pathway-dependence in NSCLC, and to validate the benefits that *SOCS-1* gene therapy could provide for NSCLC treatment in clinical practice.

Acknowledgments

This work was supported by a Grant-in-Aid from the Ministry of Health, Labour and Welfare, Japan (T. Naka) and a grant from the Kansai Biomedical Cluster Project in Saito, which is promoted by the Knowledge Cluster Initiative of the Ministry of Education, Culture, Sports, Science and Technology, Japan (T. Naka). The authors are grateful to Ms. M. Urase for experimental assistance and Ms. Y. Kanazawa and Ms. J. Yamagishi for secretarial assistance.

Disclosure Statement

The authors have no conflict of interest.

Abbreviations

AdSOCS-1	adenovirus vector containing SOCS-1
EGFR	epidermal growth factor receptor
FAK	focal adhesion kinase
LC	lung cancer
NSCLC	non-small-cell lung cancer
SOCS	suppressor of cytokine signaling
STAT	signal transducer and activator of transcription
TYK	tyrosine kinase

References

1 Hattori M, Fujita M, Ito Y, Ioka A, Katanoda K, Nakamura Y. Use of a population-based cancer registry to calculate twenty-year trends in cancer incidence and mortality in Fukui Prefecture. *J Epidemiol* 2010; **20**: 244–52.
2 Goffin J, Lacchetti C, Ellis PM, Ung YC, Evans WK. First-line systemic chemotherapy in the treatment of advanced non-small cell lung cancer: a systematic review. *J Thorac Oncol* 2010; **5**: 260–74.
3 Rossi A, Di Maio M, Chiodini P *et al.* Carboplatin- or cisplatin-based chemotherapy in first-line treatment of small-cell lung cancer: the COCIS meta-analysis of individual patient data. *J Clin Oncol* 2012; **30**: 1692–8.
4 Gao SP, Mark KG, Leslie K *et al.* Mutations in the EGFR kinase domain mediate STAT3 activation via IL-6 production in human lung adenocarcinomas. *J Clin Invest* 2007; **117**: 3846–56.
5 Lai SY, Johnson FM. Defining the role of the JAK-STAT pathway in head and neck and thoracic malignancies: implications for future therapeutic approaches. *Drug Resist Updat* 2010; **13**: 67–78.
6 Song L, Rawal B, Nemeth JA, Haura EB. JAK1 activates STAT3 activity in non-small-cell lung cancer cells and IL-6 neutralizing antibodies can suppress JAK1-STAT3 signaling. *Mol Cancer Ther* 2011; **10**: 481–94.
7 Guo Y, Xu F, Lu T, Duan Z, Zhang Z. Interleukin-6 signaling pathway in targeted therapy for cancer. *Cancer Treat Rev* 2012; **38**: 904–10.
8 Jiang R, Jin Z, Liu Z, Sun L, Wang L, Li K. Correlation of activated STAT3 expression with clinicopathologic features in lung adenocarcinoma and squamous cell carcinoma. *Mol Diagn Ther* 2011; **15**: 347–52.
9 Verstovsek S, Kantarjian H, Mesa RA *et al.* Safety and efficacy of INCB018424, a JAK1 and JAK2 inhibitor, in myelofibrosis. *N Engl J Med* 2010; **363**: 1117–27.
10 Naka T, Narazaki M, Hirata M *et al.* Structure and function of a new STAT-induced STAT inhibitor. *Nature* 1997; **387**: 924–9.
11 Starr R, Willson TA, Viney EM *et al.* A family of cytokine-inducible inhibitors of signalling. *Nature* 1997; **387**: 917–21.
12 Endo TA, Masuhara M, Yokouchi M *et al.* A new protein containing an SH2 domain that inhibits JAK kinases. *Nature* 1997; **387**: 921–4.
13 Piessevaux J, Lavens D, Peelman F, Tavernier J. The many faces of the SOCS box. *Cytokine Growth Factor Rev* 2008; **19**: 371–81.
14 Yoshimura A, Suzuki M, Sakaguchi R, Hanada T, Yasukawa H. SOCS, Inflammation, and Autoimmunity. *Front Immunol* 2012; **3**: 20.
15 Narazaki M, Fujimoto M, Matsumoto T *et al.* Three distinct domains of SSI-1/SOCS-1/JAB protein are required for its suppression of interleukin 6 signaling. *Proc Natl Acad Sci USA* 1998; **95**: 13130–4.
16 Yasukawa H, Misawa H, Sakamoto H *et al.* The JAK-binding protein JAB inhibits Janus tyrosine kinase activity through binding in the activation loop. *EMBO J* 1999; **18**: 1309–20.
17 Valentino L, Pierre J. JAK/STAT signal transduction: regulators and implication in hematological malignancies. *Biochem Pharmacol* 2006; **71**: 713–21.
18 Naka T, Fujimoto M, Tsutsui H, Yoshimura A. Negative regulation of cytokine and TLR signalings by SOCS and others. *Adv Immunol* 2005; **87**: 61–122.
19 Yoshimura A, Naka T, Kubo M. SOCS proteins, cytokine signalling and immune regulation. *Nat Rev Immunol* 2007; **7**: 454–65.
20 Zhang J, Li H, Yu JP, Wang SE, Ren XB. Role of SOCS1 in tumor progression and therapeutic application. *Int J Cancer* 2012; **130**: 1971–80.
21 Iwahori K, Serada S, Fujimoto M *et al.* Overexpression of SOCS3 exhibits preclinical antitumor activity against malignant pleural mesothelioma. *Int J Cancer* 2011; **129**: 1005–17.
22 Souma Y, Nishida T, Serada S *et al.* Antiproliferative effect of SOCS-1 through the suppression of STAT3 and p38 MAPK activation in gastric cancer cells. *Int J Cancer* 2012; **131**: 1287–96.
23 Iwahori K, Serada S, Fujimoto M *et al.* SOCS-1 gene delivery cooperates with cisplatin plus pemetrexed to exhibit preclinical antitumor activity against malignant pleural mesothelioma. *Int J Cancer* 2013; **132**: 459–71.
24 Baltayiannis G, Baltayiannis N, Tsianos EV. Suppressors of cytokine signaling as tumor repressors. Silencing of SOCS3 facilitates tumor formation and growth in lung and liver. *J BUON* 2008; **13**: 263–5.
25 Zhang S, Guo D, Jiang L, Zhang Q, Qiu X, Wang E. SOCS3 inhibiting migration of A549 cells correlates with PYK2 signaling in vitro. *BMC Cancer* 2008; **8**: 150.

doi: 10.1111/cas.12266

26 Lin YC, Lin CK, Tsai YH *et al.* Adenovirus-mediated SOCS3 gene transfer inhibits the growth and enhances the radiosensitivity of human non-small cell lung cancer cells. *Oncol Rep* 2010; **24**: 1605–12.
27 Mizuguchi H, Kay MA. A simple method for constructing E1- and E1/E4-deleted recombinant adenoviral vectors. *Hum Gene Ther* 1999; **10**: 2013–7.
28 Sakurai H, Tashiro K, Kawabata K *et al.* Adenoviral expression of suppressor of cytokine signaling-1 reduces adenovirus vector-induced innate immune responses. *J Immunol* 2008; **180**: 4931–8.
29 Verma A, Kambhampati S, Parmar S, Platanias LC. Jak family of kinases in cancer. *Cancer Metastasis Rev* 2003; **22**: 423–34.
30 Schmidmaier R, Baumann P. ANTI-ADHESION evolves to a promising therapeutic concept in oncology. *Curr Med Chem* 2008; **15**: 978–90.
31 Liu E, Cote JF, Vuori K. Negative regulation of FAK signaling by SOCS proteins. *EMBO J* 2003; **22**: 5036–46.
32 Kornberg LJ, Grant MB. Adenoviruses increase endothelial cell proliferation, migration, and tube formation: partial reversal by the focal adhesion kinase inhibitor, FRNK. *Microvasc Res* 2007; **73**: 157–62.
33 Quesnelle KM, Boehm AL, Grandis JR. STAT-mediated EGFR signaling in cancer. *J Cell Biochem* 2007; **102**: 311–9.
34 Zhang D, Takigawa N, Ochi N *et al.* Detection of the EGFR mutation in exhaled breath condensate from a heavy smoker with squamous cell carcinoma of the lung. *Lung Cancer* 2011; **73**: 379–80.
35 Lai JM, Chang JT, Wen CL, Hsu SL. Emodin induces a reactive oxygen species-dependent and ATM-p53-Bax mediated cytotoxicity in lung cancer cells. *Eur J Pharmacol* 2009; **623**: 1–9.
36 Amin AR, Wang D, Zhang H *et al.* Enhanced anti-tumor activity by the combination of the natural compounds (-)-epigallocatechin-3-gallate and luteolin: potential role of p53. *J Biol Chem* 2010; **285**: 34557–65.
37 Oh HL, Lee DK, Lim H, Lee CH. HY253, a novel decahydrofluorene analog, from Aralia continentalis, induces cell cycle arrest at the G1 phase and cytochrome c-mediated apoptosis in human lung cancer A549 cells. *J Ethnopharmacol* 2010; **129**: 135–9.
38 Yamada C, Ozaki T, Ando K *et al.* RUNX3 modulates DNA damage-mediated phosphorylation of tumor suppressor p53 at Ser-15 and acts as a co-activator for p53. *J Biol Chem* 2010; **285**: 16693–703.
39 Nagai Y, Miyazawa H, Huqun *et al.* Genetic heterogeneity of the epidermal growth factor receptor in non-small cell lung cancer cell lines revealed by a rapid and sensitive detection system, the peptide nucleic acid-locked nucleic acid PCR clamp. *Cancer Res* 2005; **65**: 7276–82.
40 Zimmer S, Kahl P, Buhl TM *et al.* Epidermal growth factor receptor mutations in non-small cell lung cancer influence downstream Akt, MAPK and Stat3 signaling. *J Cancer Res Clin Oncol* 2009; **135**: 723–30.
41 Kashii T, Mizushima Y, Monno S, Nakagawa K, Kobayashi M. Gene analysis of K-, H-ras, p53, and retinoblastoma susceptibility genes in human lung cancer cell lines by the polymerase chain reaction/single-strand conformation polymorphism method. *J Cancer Res Clin Oncol* 1994; **120**: 143–8.
42 Mallette FA, Calabrese V, Ilangumaran S, Ferbeyre G. SOCS1, a novel interaction partner of p53 controlling oncogene-induced senescence. *Aging (Albany NY)* 2010; **2**: 445–52.

Supporting Information

Additional supporting information may be found in the online version of this article:

Data S1. Methods.

OPEN ACCESS Freely available online

PLOS | ONE

Karyopherin Alpha2 Is Essential for rRNA Transcription and Protein Synthesis in Proliferative Keratinocytes

Noriko Umegaki-Arao[1], Katsuto Tamai[2]*, Keisuke Nimura[3], Satoshi Serada[4], Tetsuji Naka[4], Hajime Nakano[5], Ichiro Katayama[1]

1 Department of Dermatology, Osaka University Graduate School of Medicine, Osaka, Japan, **2** Department of Stem Cell Therapy Science, Osaka University Graduate School of Medicine, Osaka, Japan, **3** Division of Gene Therapy Science, Osaka University Graduate School of Medicine, Osaka, Japan, **4** National Institute of Biomedical Innovation Laboratory for Immune Signal, Osaka, Japan, **5** Department of Dermatology, Hirosaki University School of Medicine, Hirosaki, Japan

Abstract

Karyopherin proteins mediate nucleocytoplasmic trafficking and are critical for protein and RNA subcellular localization. Recent studies suggest KPNA2 expression is induced in tumor cells and is strongly associated with prognosis, although the precise roles and mechanisms of KPNA2 overexpression in proliferative disorders have not been defined. We found that KPNA2 expression is induced in various proliferative disorders of the skin such as psoriasis, Bowen's disease, actinic keratosis, squamous cell carcinoma, Paget's disease, Merkel cell carcinoma, and mycosis fungoides. siRNA-mediated KPNA suppression revealed that KPNA2 is essential for significant suppression of HaCaT proliferation under starvation conditions. Ribosomal RNA transcription and protein synthesis were suppressed by starvation combined with knockdown of KPNA (including KPNA2) expression. KPNA2 localized to the nucleolus and interacted with proteins associated with mRNA processing, ribonucleoprotein complex biogenesis, chromatin modification, and transcription, as demonstrated by tandem affinity purification and mass spectrometry. KPNA2 may be an important promoter of ribosomal RNA and protein synthesis in tumor cells.

Citation: Umegaki-Arao N, Tamai K, Nimura K, Serada S, Naka T, et al. (2013) Karyopherin Alpha2 Is Essential for rRNA Transcription and Protein Synthesis in Proliferative Keratinocytes. PLoS ONE 8(10): e76416. doi:10.1371/journal.pone.0076416

Editor: Andrzej T. Slominski, University of Tennessee, United States of America

Received November 9, 2012; **Accepted** August 29, 2013; **Published** October 3, 2013

Funding: This work was supported by a Grant-in-Aid of Scientific Research from the Ministry of Education, Culture, Science and Technology of Japan, and a Health and Labour Science Research Grant from the Ministry of Health, Labour and Welfare of Japan. The funders had no role in study design, data collection and analysis, decision to publish, or preparation of the manuscript.

Competing Interests: The authors have declared that no competing interests exist.

* E-mail: tamai@gts.med.osaka-u.ac.jp

Introduction

Recent studies have defined the molecular mechanisms of nucleocytoplasmic signal transduction by karyopherins (KPNs), which function as receptors for various intracellular molecules and mediate nuclear import and export during interphase. In humans, the karyopherin alpha (KPNA) family consists of at least 7 family members, all of which interact with karyopherin beta (KPNB) 1 and transport various proteins and RNAs through the nuclear pores in an energy-dependent manner [1–3]. Various extracellular environmental changes activate intracellular signaling cascades by which cells exchange activated signaling molecules between the nucleus and cytoplasm via the KPN-mediated machinery to regulate proliferation and differentiation status [2,4–6]. KPNA2 expression in human epidermal keratinocytes, but not in human dermal fibroblasts, is differentially regulated by transforming growth factor (TGF)-β_1 and interferon (IFN)-γ, both of which are established modulators of epidermal proliferation and differentiation [4]. KPNA2 also mediates the translocation of epidermal differentiation-inducing signals into the nucleus by recruiting transcription factors such as interferon regulatory factor-1 (IRF-1), thereby inducing IFN-γ-mediated epidermal differentiation [4]. Karyopherin alphas also mediate mitotic spindle assembly [7–9] and nuclear membrane formation [10]. KPNB1 is also a global regulator of mitotic spindle assembly, centrosome dynamics, nuclear membrane formation, and nuclear pore complex assembly [11,12]. Recent studies have revealed that KPNs including KPNA2 are overexpressed in various kinds of tumors such as breast cancer, cervical cancer, non-small cell lung cancer, prostate cancer, and primary cutaneous melanoma, and that expression levels in these tumors are closely associated with prognosis [13–18]. Nevertheless, the precise roles and mechanisms of KPN overexpression in proliferative disorders have not been defined.

The rate of cell growth and proliferation is proportional to the rate of protein synthesis, which is tightly linked to ribosome biologics [19,20]. RNA synthesis and ribosome construction occur in the nucleolus and their control is important for regulating protein synthesis; however, the precise mechanisms and roles of karyopherins in regulating rRNA and protein synthesis remain unclear.

We report KPNA2 induction in proliferation disorders regardless of malignancy, and suggest KPNA2 regulates rRNA transcription and general protein synthesis in the nucleolus to maintain proliferation.

Materials and Methods

Skin Samples

Written informed consent was obtained from all patients, and the study protocol was approved by Medical Ethics Committee of Osaka University.

Cell Culture

HaCaT cells, an immortalized, nontumorigenic keratinocyte cell line, were cultured in Dulbecco's modified Eagle's medium (DMEM; Nacalai Tesque) containing 10% fetal bovine serum (FBS) at 37°C under 5% CO_2-95% air.

RNA Purification and Reverse Transcription-quantitative Polymerase Chain Reaction

Total RNA was isolated from HaCaT cells with an RNA isolation kit (Qiagen) and reverse transcribed with SuperScript III reverse transcriptase (Invitrogen). Expression of pre-rRNA was determined by using Power SYBR green PCR Master Mix (Applied Biosystems) according to the manufacturer's protocol. β-Actin was used to normalize target gene expression. PCR amplification was performed with 5′-ATCGTCCACCGCAAATGCTTCTA-3′ and 5′-AGCCATGCCAATCTCATCTTGTT-3′ for β-actin and 5′-GAACGGTGGTGTGTCGTTC-3′ and 5′-GCGTCTCGTCTCGTCTCACT-3′ for pre-rRNA [21]. PCR cycling conditions were 40 cycles of denaturing at 92°C for 15 sec and annealing at 60°C for 60 sec on an ABI Prism 7000 sequence detection system (Applied Biosystems).

Small Interfering RNA and Plasmid DNA Transfection

Small interfering RNAs (siRNAs) specific for KPNA1, 2, 3, and 4 and the control stealth siRNA were obtained from Invitrogen. Cells (1.5×10^6) were transfected with 100 ng siRNAs mixture using the Neon transfection system (Invitrogen). We performed the knockdown studies with each siRNA, which ensured more than 50–70% suppression of KPNA2 mRNA and protein.

MTS

[3-(4,5-dimethylthiazol-2-yl)-5(3-carboxymethoxyphenyl)-2-(4-sulfophenyl)-2H-tetrazolium] assay. HaCaT cells induced with each siRNA were seeded at their optimal cell density (7×10^4 cells/well) in 96-well microtiter plates and incubated to allow cell attachment. After 6 h, cells were incubated with 0.1% FBS DMEM for 24, 48, 72, and 120 h. At the end of each incubation period, cell viability was determined by using the CellTiter 96® AQ_{ueous} Non-Radioactive Cell Proliferation Assay (Promega) according to the manufacturer's instructions. Samples were incubated at 37°C in a humidified 5% CO_2 atmosphere for 1 h. Absorbance was measured at 490 nm using a microplate reader.

Immunohistochemistry

Slides of skin biopsies in paraffin blocks were stained with hematoxylin and eosin (HE) and anti-human KPNA2 mouse monoclonal antibody (BD Biosciences) (1:1000).

Immunofluorescence

HaCaT cells were fixed in 4% formaldehyde in phosphate-buffered saline (PBS) for 40 min. After rinsing twice with PBS, the cells were permeabilized in 0.5% Triton X-100 in PBS for 60 s and blocked with 2% skim milk overnight at 4°C. The cells were incubated with anti-UBF (Santa Cruz) and anti-KPNA2 antibodies for 1 h and stained with Alexa Fluor 546 goat anti-rabbit IgG and Alexa Fluor 488 goat anti-mouse IgG secondary antibodies (1:1000; Invitrogen A-11035 and A-11029) for 1 h. After washing with PBS, cells were counterstained with 0.5 mg/mL 4′, 6′-diamidino-2-phenylindole (DAPI) and mounted with Vectashield mounting medium (Vector Laboratories). Cells were analyzed using a Radiance 2100 confocal scanning-laser microscope (Bio-Rad) equipped with an Eclipse TE-2000 inverted microscope (Nikon) or a Nikon A1 confocal scanning-laser microscope equipped with a Nikon Eclipse Ti inverted microscope.

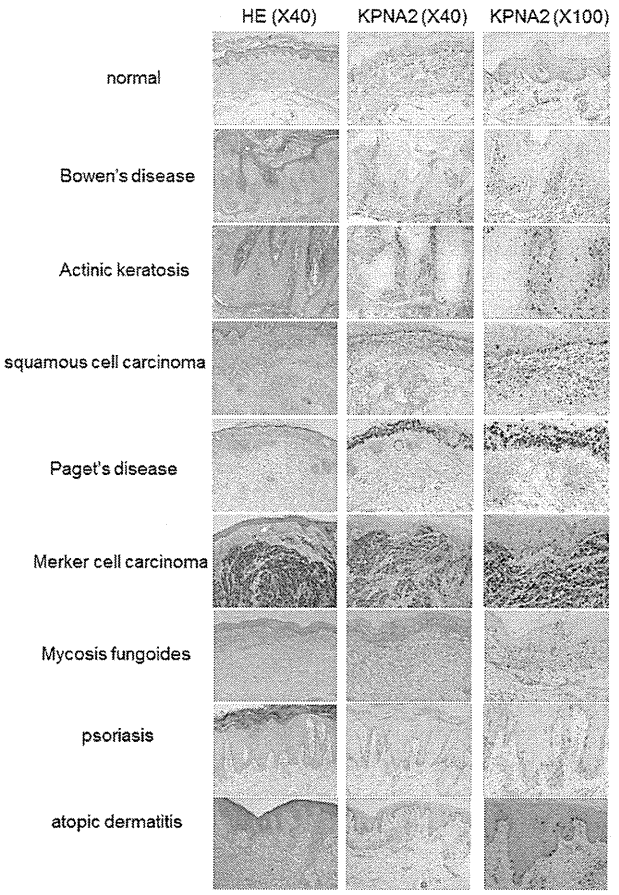

Figure 1. Overexpression of KPNA2 in proliferating cells. Immunohistochemistry showed KPNA2 was uniformly expressed throughout the epidermis in healthy skin, although KPNA2 overexpression was observed in the basal layer in psoriasis. In contrast, very few cells exhibited KPNA2 staining in the basal cells of atopic dermatitis. KPNA2 overexpression was observed in the tumor cells of Bowen's disease, actinic keratosis, squamous cell carcinoma, Paget's disease, Merkel cell carcinoma, and mycosis fungoides.
doi:10.1371/journal.pone.0076416.g001

Tandem Affinity Purification (TAP) and Mass Spectrometry

KPNA2 and GFP cDNAs were introduced into pCAGIP-gw-TAP by using Gateway technology (Invitrogen). KPNA2-TAP and GFP-TAP complexes were purified from HaCaT cell extracts using TAP technology [22,23]. Proteins were separated by SDS-PAGE and stained with the Silver Stain MS Kit (Wako Pure Chemical Industries). Protein bands were excised from the gel and digested with trypsin (Promega) [24]. NanoLC-MS/MS analyses were performed on a LTQ-Orbitrap XL mass spectrometer (Thermo Fisher Scientific) equipped with a nano-ESI source (AMR) and coupled to a Paradigm MG4 pump (Michrom Bioresources) and an autosampler (HTC PAL, CTC Analytics). A spray voltage of 1800 V was applied. The peptide mixture was separated on a MagicC18AQ column (100 μm×150 mm, 3.0 μm particle size, 300 Å, Michrom Bioresources) with a flow rate of 500 nl/min. A linear gradient of 5% to 45% B in 30 min, 45% to 95% B in 0.1 min, and 95% B for 2 min and 5% B was employed

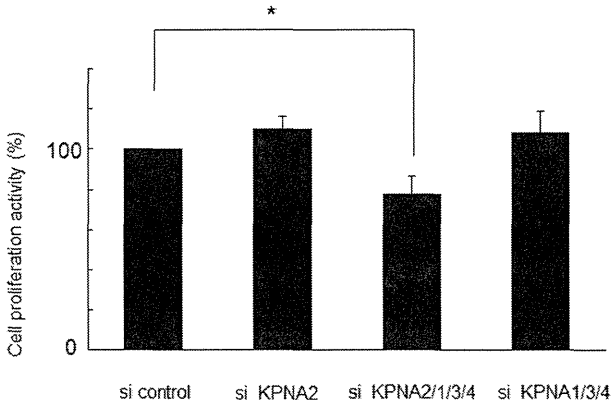

Figure 2. Suppression of cell growth by combined KPNA knockdown. Under starvation conditions (0.1% FBS), siRNA-mediated knockdown of KPNA2, 1, 3, and 4 suppressed cell growth after 120 h (*$p<0.05$). Only KPNA2 siRNA subtraction produced no change in proliferation.
doi:10.1371/journal.pone.0076416.g002

(A = 0.1% formic acid in 2% acetonitrile, B = 0.1% formic acid in 90% acetonitrile). Intact peptides were detected in the Orbitrap at 60,000 resolutions. For LC-MS/MS analysis, 6 precursor ions were selected for MS/MS scans in a data-dependent acquisition mode following each full scan (m/z, 350–1500). A lock mass function was used for the LTQ-Orbitrap to obtain constant mass accuracy during gradient analysis.

Peptides and proteins were identified by automated database searching the Swiss-Prot protein database (version 57.14x) with the MASCOT search program (version 1.0; Matrix Science) and a precursor mass tolerance of 10 p.p.m., a fragment ion mass tolerance of 0.8 Da, and strict trypsin specificity, allowing for up to 2 missed cleavages. Carbamidomethylation of cysteine was set as a fixed modification and oxidation of methionines was allowed as a variable modification.

Metabolic Labeling

HaCaT cells were labeled for 2 h with 100 mCi ^{35}S-methionine in methionine-free DMEM (Gibco) supplemented with 10% dialyzed serum. Protein was extracted with TNE buffer containing 50 mM Tris-HCl at pH 7.4, 150 mM NaCl, 2 mM EDTA, and 0.5% NP-40, then resuspended in 1% sodium dodecyl sulfate and boiled for 10 min at 100°C. Radioactivity was measured with a Beckmann Coulter liquid scintillation counter and normalized to protein content.

Transient Transfection and Luciferase Assay

The human pre-rRNA-luc vector was kindly provided by Dr. Samson Jacob [25]. HaCaT cells induced with each siRNA were seeded in a 12-well plate and transfected with 0.34 μg human-pre-rRNA-luc plasmid and Fugene 6 transfection reagent (Roche). The luciferase reporter assay was performed using a commercial luciferase assay kit (Promega). Data were normalized to the protein concentration.

Statistical Analysis

All data and results were confirmed in at least 3 independent experiments. Statistical significance was determined by one-way analysis of variance (ANOVA).

Results

KPNA2 Overexpression in Proliferative Disorders of the Skin

To investigate KPNA2 expression in various epidermal-proliferative disorders of the skin, immunohistochemical staining of KPNA2 was performed on biopsy specimens of epidermal tumors as well as psoriasis and atopic dermatitis, which are inflammatory skin diseases with higher and lower epidermal proliferation, respectively. KPNA2 staining was faint and homogeneous without significant nuclear accumulation in healthy epidermis. In contrast, there was marked KPNA2 staining in the nuclei and cytoplasm of malignant cells in several skin tumors with different prognoses including Bowen's disease, actinic keratosis, squamous cell carcinoma (SCC), Paget's disease, Merkel cell carcinoma, and Mycosis fungoides. In malignant cells of SCC *in situ* such as Bowen's disease and actinic keratosis as with well prognosis, KPNA2 expressed predominantly in the basal layer. In contrast, established SCC showed rather intense and diffuse expression of KPNA2 in the malignant cells. Non-squamous cell malignant tumors of the skin including Paget's disease, Merkel cell carcinoma, and mycosis fungoides also showed diffuse, intense staining of KPNA2, indicating significantly higher expression in skin malignancy. Marked staining of KPNA2 was also observed in psoriatic skin, but was limited to the cytoplasm of basal layer keratinocytes. In contrast, very few but significant numbers of KPNA2-positive keratinocytes were observed in the basal lesions of atopic dermatitis, particularly in the inflamed proliferating lesions (**Figure 1**).

Contribution of KPNA2 and other KPNAs to Keratinocyte Cell Growth

To assess the role of KPNs in keratinocyte proliferation, HaCaT cell growth in culture was assessed by MTS assay after siRNA-mediated knockdown of KPNs. In culture medium containing 10% FBS, growth was significantly suppressed by KPNB1 knockdown [13]; however, knockdown of other KPNAs produced no significant effect (data not shown). In starved culture medium with 0.1% FBS, HaCaT cell growth was significantly suppressed by siRNA knockdown of KPNA1, 2, 3, and 4, suggesting adequate expression of KPNAs may be required for growth maintenance, especially in starved cells such as cancer cells. About 20% of HaCaT keratinocyte growth was suppressed 120 h after KPNA knockdown. KPNA siRNAs were individually subtracted from the siRNA cocktail to investigate the contribution of each KPNA to growth suppression. Interestingly, only KPNA2 siRNA subtraction resulted in the significant recovery of cell growth up to the control level (**Figure 2**), while removal of the other KPNA siRNAs did not affect growth suppression (data not shown). KPNA2 knockdown alone had no significant growth suppression effect, suggesting the other KPNAs are redundant. These data suggest KPNAs complement each other during cell growth, but KPNA2 may be essential for maintaining cell proliferation under starvation conditions.

Association of KPNA2 with Ribosomal Proteins in the Nucleolus

To identify proteins that interact with KPNA2 in HaCaT keratinocytes, we used the TAP method, which enabled us to easily isolate and purify proteins bound to the stably expressed TAP-tagged target recombinant protein [22,23]. Proteins associated with the KPNA2-TAP complex were isolated from the nuclei and cytoplasm of KPNA2-TAP-expressing HaCaT cells, separated

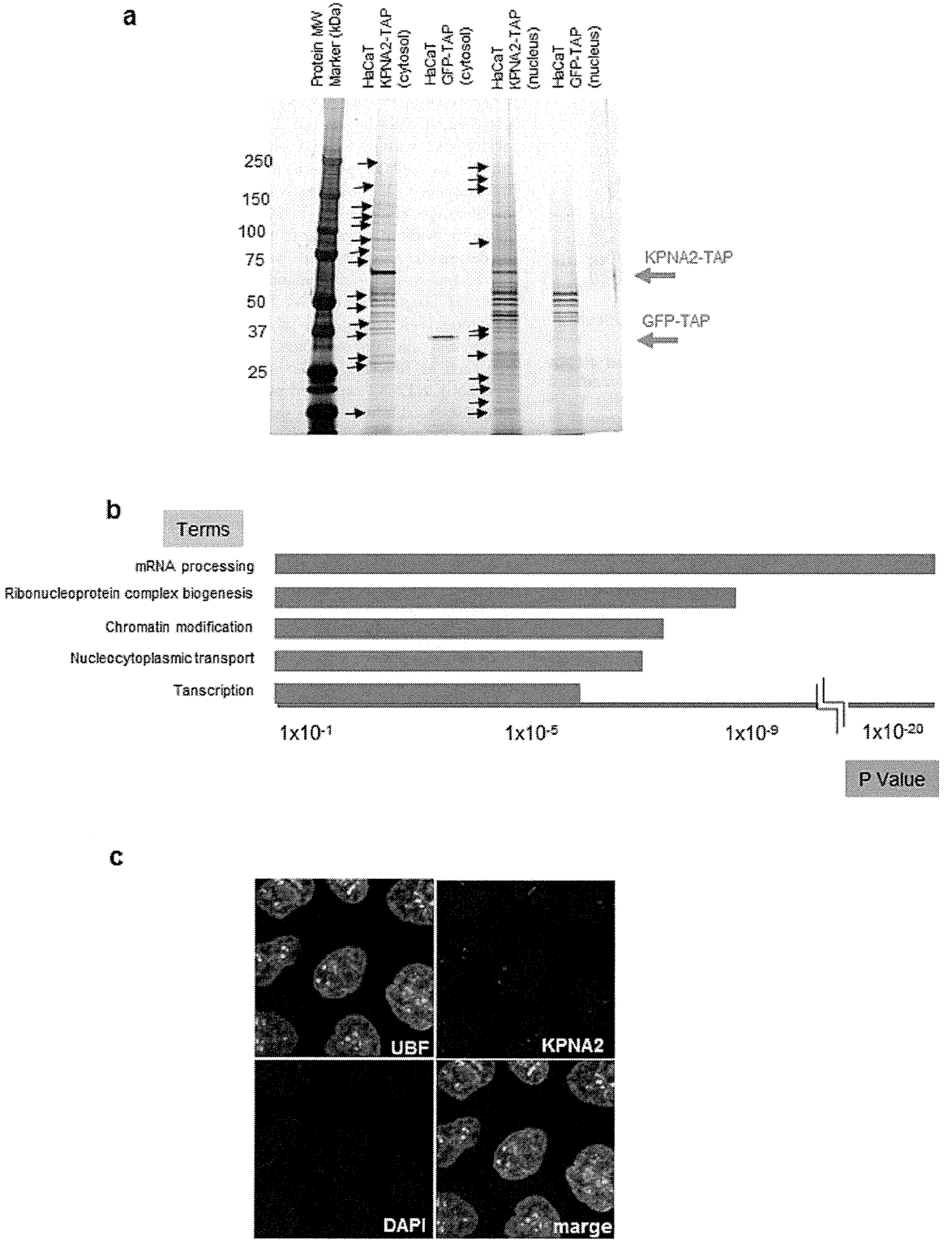

Figure 3. Detection and analysis of proteins that interact with KPNA2 and localization of KPNA2 in the nucleolus. Proteins that interact with KPNA2 in the cytoplasm and nucleus were purified using the TAP method and detected by silver staining. Proteins marked with arrows were analyzed by LC/MS/MS. HaCaT cells expressing GFP-TAP were used to detect nonspecific interactions. **a)** The results of LC/MS/MS were analyzed by pathway analysis using reactome (http://www.reactome.org). The categories of "mRNA processing", "ribonucleoprotein complex biogenesis", "chromatin modification," and "transcription" were the most significantly represented pathways. **b)** Immunohistochemistry revealed KPNA2 co-localization with UBF, a nucleolar marker.
doi:10.1371/journal.pone.0076416.g003

Table 1. Lists of proteins analyzed by pathway analysis.

mRNA processing	
RALY	RNA-binding protein Raly
NCBP1	Nuclear cap-binding protein subunit 1
RNMT	mRNA cap guanine-N7 methyltransferase
GAR1	H/ACA ribonucleoprotein complex subunit 1
PABPC4	PABPC4 protein
MLH1	DNA mismatch repair protein Mlh1
YBX1	Nuclease-sensitive element-binding protein 1
SRRT	Serrate RNA effector molecule homolog
DDX17	Probable ATP-dependent RNA helicase DDX17
RRP1B	Ribosomal RNA processing protein 1 homolog B
PCBP1	Poly(rC)-binding protein 1
PCBP2	Poly(rC)-binding protein 2
SFRS9	Splicing factor, arginine/serine-rich 9
PABPC1	Polyadenylate-binding protein 1
NSUN2	tRNA (cytosine-5-)-methyltransferase NSUN2
KRR1	KRR1 small subunit processome component homolog
DHX9	ATP-dependent RNA helicase A
RRP1	Ribosomal RNA processing protein 1 homolog B
DDX1	ATP-dependent RNA helicase DDX1
HNRNPU	Heterogeneous nuclear ribonucleoprotein U
TTF2	Transcription termination factor 2
SFRS3	Splicing factor, arginine/serine-rich 3
PHAX	Phosphorylated adapter RNA export protein
NOP2	Putative ribosomal RNA methyltransferase NOP2
RPS16	RPS16 protein
SNRNP200	U5 small nuclear ribonucleoprotein 200 kDa helicase
SYF2	Pre-mRNA-splicing factor SYF2
NOP56	NOP56 protein
RBM14	RNA-binding protein 14
BAT1	Spliceosome RNA helicase BAT1
ADAR	Double-stranded RNA-specific adenosine deaminase
KIAA1429	Protein virilizer homolog
Ribonucleoprotein complex biogenesis	
NCBP1	Nuclear cap-binding protein subunit 1
KRR1	KRR1 small subunit processome component homolog
RRP1	Ribosomal RNA processing protein 1 homolog B
GAR1	H/ACA ribonucleoprotein complex subunit 1
NIP7	60 S ribosome subunit biogenesis protein NIP7 homolog
DDX1	ATP-dependent RNA helicase DDX1
PHAX	Phosphorylated adapter RNA export protein
NOP2	Putative ribosomal RNA methyltransferase NOP2
RPS16	RPS16 protein
RRP1B	Ribosomal RNA processing protein 1 homolog B
SNRNP200	U5 small nuclear ribonucleoprotein 200 kDa helicase
SFRS9	Splicing factor, arginine/serine-rich 9
NOP56	NOP56 protein
Chromatin modification	

Table 1. Cont.

mRNA processing	
ING5	Inhibitor of growth protein 5
RBBP4	Histone-binding protein RBBP4
RBBP7	Histone-binding protein RBBP7
ARID2	AT-rich interactive domain-containing protein 2
CHD8	Chromodomain-helicase-DNA-binding protein 8
HDAC2	Histone deacetylase 2
HDAC1	Histone deacetylase 1
ASH1L	Probable histone-lysine N-methyltransferase ASH1L
BRDT	Bromodomain testis-specific protein
RBM14	RNA-binding protein 14
BCOR	BCL-6 corepressor
CHD4	Chromodomain-helicase-DNA-binding protein 4
MLL2	Histone-lysine N-methyltransferase MLL2
Nucleocytoplasmic transport	
PHAX	Phosphorylated adapter RNA export protein
NCBP1	Nuclear cap-binding protein subunit 1
UPF1	Regulator of nonsense transcripts 1
SET	Protein SET
GLE1	Nucleoporin GLE1
NUPL2	Nucleoporin-like protein 2
TPR	Nucleoprotein
KPNA2	Importin subunit alpha-2
KPNB1	Importin subunit beta-1
BAT1	Spliceosome RNA helicase BAT1
Transcription	
ING5	Inhibitor of growth protein 5
NMI	N-myc-interactor
FOXK1	Forkhead box protein K1
FOXM1	Forkhead box protein M1
CCNT1	Cyclin-T1
ARID2	AT-rich interactive domain-containing protein 2
YBX1	Nuclease-sensitive element-binding protein 1
CNOT4	CCR4-NOT transcription complex subunit 4
YBX2	Y-box-binding protein 2
CHD8	Chromodomain-helicase-DNA-binding protein 8
ASH2L	Set1/Ash2 histone methyltransferase complex subunit ASH2
BCOR	BCL-6 corepressor
EWSR1	RNA-binding protein EWS
CHD4	Chromodomain-helicase-DNA-binding protein 4
MLL2	Histone-lysine N-methyltransferase MLL2
ASXL3	Putative Polycomb group protein ASXL3
TAF4	Transcription initiation factor TFIID subunit 4
RBBP4	Histone-binding protein RBBP4
TAF6	Transcription initiation factor TFIID subunit 6
POLR1A	DNA-directed RNA polymerase I subunit RPA1
MED12	Mediator of RNA polymerase II transcription subunit 12
CSDA	DNA-binding protein A

doi:10.1371/journal.pone.0076416.t001

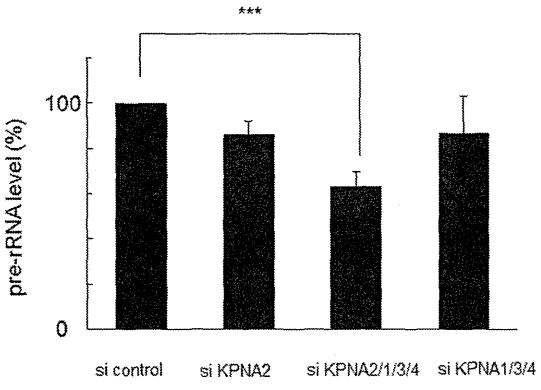

Figure 4. Suppression of ribosomal RNA synthesis by combined KPNA knockdown. Under starvation conditions (0.1% fetal bovine serum), siRNA-mediated knockdown of KPNA2, 1, 3, and 4 significantly suppressed ribosomal RNA synthesis analyzed by reverse transcription-quantitative polymerase chain reaction (***p<0.01). The amount of pre-ribosomal RNA was reduced by about 37% after 72 h.
doi:10.1371/journal.pone.0076416.g004

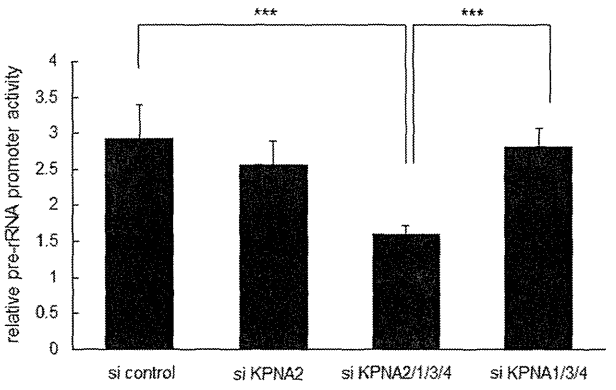

Figure 6. Suppression of the pre-ribosomal RNA promoter by combined KPNA knockdown. Under starvation conditions (0.1% fetal bovine serum), siRNA-mediated knockdown of KPNA2, 1, 3, and 4 significantly suppressed pre-rRNA promoter activity after 24 h (***p<0.01).
doi:10.1371/journal.pone.0076416.g006

by SDS-PAGE, and silver stained. HaCaT cells expressing GFP-TAP were used as a negative control (**Figure 3a**). KPNA2-TAP-associated proteins extracted from the silver-stained gel were identified by mass spectrometry. Numerous proteins were analyzed by reactome (http://www.reactome.org) to investigate their biological relationships. Pathway analysis revealed that the proteins interacting with KPNA2 were associated with mRNA processing, ribonucleoprotein complex biogenesis, chromatin modification, and transcription, all of which are essential for cell activities including cell growth (**Figure 3b, Table 1**). Interestingly, significant numbers of ribosomal proteins were listed as associated with KPNA2. Furthermore, immunofluorescence staining of KPNA2 in cultured HaCaT keratinocytes demonstrated co-localization of KPNA2 with UBF in the nucleoli, suggesting a role of KPNA2 for maintaining rRNA function (**Figure 3c**).

Contribution of KPNA2 to Protein Synthesis and Ribosomal RNA Transcription

Because the nucleolus is specifically responsible for rRNA transcription and maintenance of gene expression/transcription and mRNA processing, we hypothesized that KPNA2 in the nucleoli may regulate rRNA transcription to maintain cell growth under starvation conditions. To test this hypothesis, the siRNA cocktail was again applied to knockdown KPNAs to observe the effect on pre-rRNA transcription in starved HaCaT keratinocytes. Knockdown of all KPNAs reduced pre-rRNA levels as measured by RT-qPCR. In the 72 h after treatment with the siRNA cocktail, pre-rRNA expression was reduced by about 40%. Subtraction of KPNA2 siRNA restored pre-rRNA expression. The other KPNAs did not contribute to pre-rRNA expression. Treatment with KPNA2 siRNA alone had no significant effect, suggesting a redundant mechanism with other KPNAs (**Figure 4**). Protein synthesis in HaCaT keratinocytes was also reduced, corresponding to the suppression of pre-rRNA expression (**Figure 5**). The pre-rRNA promoter was also suppressed by KPNA knockdown after 24 h (**Figure 6**). Fluorescence-activated cell sorting of HaCaT cells before and after KPNA knockdown showed no significant change in the cell cycle pattern (data not shown). These data suggest KPNA2 might positively regulate rRNA transcription in the nucleolus, maintaining cell growth by ensuring transcription and translation directly or indirectly.

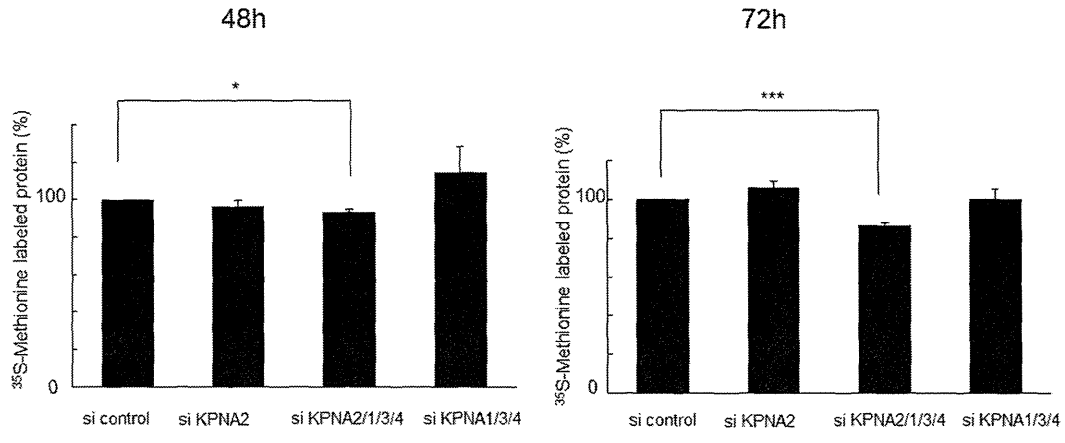

Figure 5. Suppression of protein synthesis by combined KPNA knockdown. Under starvation conditions (0.1% fetal bovine serum), siRNA-mediated knockdown of KPNA2, 1, 3, and 4 significantly suppressed protein synthesis after 48 h (*p<0.05) and 72 h (***p<0.01), as demonstrated by metabolic labeling with ^{35}S-methionine.
doi:10.1371/journal.pone.0076416.g005

Discussion

In this study, KPNA2 was overexpressed in proliferating disorders of the skin and interacted with many kinds of proteins that control transcription and gene expression directly and indirectly. This was the first report to show that KPNA2 is essential for cell growth in terms of rRNA and protein synthesis under starvation conditions.

KPNA2 overexpression in several skin malignancies is associated with varying prognoses. In the basal cells of psoriasis, KPNA2 expression was diffusely up-regulated in comparison to atopic dermatitis. Thus, KPNA2 expression might be induced in cells in which proliferation has been activated. Comparing Bowen's disease and actinic keratosis, which are known as SCC *in situ*, KPNA2 was remarkably and diffusely overexpressed. KPNA2 may therefore be a tumor marker with utility as a prognostic factor of proliferative activity in skin malignancies, although we have insufficient sample sizes to determine significance. Previous reports have demonstrated KPNA2 overexpression in various tumors cells *in vitro* and *in vivo*; elevated KPNA2 and KPNB1 expression in cancer cells correlates with altered transcriptional regulation associated with deregulated E2F/Rb activities [26]. Some studies have indicated that higher KPNA2 expression in tumor cell nuclei shortens patient survival, although the mechanisms and precise roles of KPNA2 in the tumor cells remained unclear [16,17]. Researchers also hypothesized that KPNA2-mediated nuclear transport of proteins necessary for maintaining cell proliferation, such as transcription factors, promote tumor cell growth. In this context, KPNA2 was shown to interact with NBS1 (Nijmegen breakage syndrome 1), a key regulator of the MRE11/RAD50/NBS1 complex. NBS1 promotes tumorigenesis by binding and activating the phosphatidylinositol 3-kinase/AKT pathway [27]. Interestingly, siRNA-medicated KPNA2 knockdown studies revealed a different cellular response to KPNA2 inhibition in prostate and cervical cancer cell lines. In prostate cell line PC3, proliferation and viability were significantly reduced when KPNA2 expression was inhibited, whereas there was no significant change in a cervical cancer cell line. This difference could be due to tissue-specific tumor etiologies [13,17].

In this study, we characterized KPNA2-binding proteins *in situ* in immortalized HaCaT keratinocytes. In silico gene ontology indicated a significant relationship between KPNA2 binding proteins and mRNA processing, ribonucleoprotein complex biogenesis, chromatin modification, and transcription. KPNA2 interacted with various ribosomal proteins and heterogeneous nuclear ribonucleoproteins directly or indirectly and was located in the nucleolus, the site of pre-rRNA transcription and processing and ribosome assembly. rRNA synthesis, the first event in ribosome synthesis, is a fundamental determinant of a cell's capacity to grow and proliferate. Ribosomal RNA genes (rDNAs) are transcribed with high efficiency and the complex regulation of rRNA synthesis is responsive to general metabolism and specific environmental challenges [20,28]. Serum starvation is also a well-established approach to inducing a broad range of cellular stress. TAP analysis revealed that KPNA2 associates with numerous ribosomal RNA synthesis-related proteins including RNA polymerase I subunit, rRNA methyl transferase, rRNA subunit biogenesis protein, and rRNA processing proteins. Furthermore, KPNA2 accumulates in the nucleolus and contributes to rRNA transcription *in vitro*. These lines of evidence suggest KPNA2 may serve important roles as a canonical nuclear transporter and to ensure rRNA biogenesis in proliferating cells. In this context, enhanced KPNA2 expression in malignant and inflammatory keratinocytes may positively regulate their proliferating capacity by supporting rRNA synthesis, which is indispensable. In malignant cells, the poor prognosis indicated by nuclear KPNA2 accumulation may be associated with KPNA2 retention in response to cellular stress and increasing rRNA synthesis or changing gene expression.

KPNA subtypes exhibit different abilities to interact with specific NLS-containing cargos and in various expression patterns in cells and tissues. KPNA2 is highly expressed in undifferentiated embryonic stem cells and down-regulated during neural differentiation, indicating that proper expression of KPNA2 is required for embryonic stem cells to maintain their undifferentiated state [29]. KPNs are also complementary because they are indispensable for cellular proliferation and differentiation. We previously examined the effect of KPNA2 siRNA subtraction on RNA expression in normal human keratinocytes by microarray analysis [4]; however, there was no increases of more than 2 fold in any other KPNs including KPNA1, 3, 4, and KPNB1 (data not shown).

In this study, KPNA2 was essential for cell growth related to rRNA and protein synthesis under starvation conditions; however, there was no significant change when only KPNA2 was knocked down. Combined knockdown of KPNA2, 1, 3, and 4 was needed to suppress cell growth and KPNA2 was indispensable. Even under these conditions, growth suppression was gradual and mild over 120 h. Furthermore, combined knockdown of KPNAs mildly suppressed the synthesis of rRNA and proteins after 72 h. These results indicated that KPNAs might play complementary roles with sufficient reserves.

Further studies are needed to clarify the additional function of KPNA2 in cell proliferation, which would be a focus for a new treatment to regulate KPNA2.

Acknowledgments

We sincerely appreciate the kind support of Prof. Yasufumi Kaneda. We also thank Ms. Eriko Nobuyoshi and Ms. Sayaka Matsumura for technical support with immunohistochemistry and reverse transcription-quantitative polymerase chain reaction.

Author Contributions

Conceived and designed the experiments: NU KT KN TN. Performed the experiments: NU SS. Analyzed the data: NU KT KN TN IK. Contributed reagents/materials/analysis tools: HN IK. Wrote the paper: NU KT.

References

1. Pemberton LF, Paschal BM (2005) Mechanisms of receptor-mediated nuclear import and nuclear export. Traffic 6: 187–198.
2. Yasuhara N, Oka M, Yoneda Y (2009) The role of the nuclear transport system in cell differentiation. Semin Cell Dev Biol 20: 590–599.
3. Yasuda Y, Miyamoto Y, Yamashiro T, Asally M, Masui A, et al. (2012) Nuclear retention of importin alpha coordinates cell fate through changes in gene expression. EMBO J 31: 83–94.
4. Umegaki N, Tamai K, Nakano H, Moritsugu R, Yamazaki T, et al. (2007) Differential regulation of karyopherin alpha 2 expression by TGF-beta1 and IFN-gamma in normal human epidermal keratinocytes: evident contribution of KPNA2 for nuclear translocation of IRF-1. J Invest Dermatol 127: 1456–1464.
5. Freire J, Covelo G, Sarandeses C, Diaz-Jullien C, Freire M (2001) Identification of nuclear-import and cell-cycle regulatory proteins that bind to prothymosin alpha. Biochem Cell Biol 79: 123–131.
6. Hall MN, Griffin CA, Simionescu A, Corbett AH, Pavlath GK (2011) Distinct roles for classical nuclear import receptors in the growth of multinucleated muscle cells. Dev Biol 357: 248–258.
7. Schatz CA, Santarella R, Hoenger A, Karsenti E, Mattaj IW, et al. (2003) Importin alpha-regulated nucleation of microtubules by TPX2. EMBO J 22: 2060–2070.

8. Gruss OJ, Carazo-Salas RE, Schatz CA, Guarguaglini G, Kast J, et al. (2001) Ran induces spindle assembly by reversing the inhibitory effect of importin alpha on TPX2 activity. Cell 104: 83–93.
9. Ems-McClung SC, Zheng Y, Walczak CE (2004) Importin alpha/beta and Ran-GTP regulate XCTK2 microtubule binding through a bipartite nuclear localization signal. Mol Biol Cell 15: 46–57.
10. Askjaer P, Galy V, Hannak E, Mattaj IW (2002) Ran GTPase cycle and importins alpha and beta are essential for spindle formation and nuclear envelope assembly in living Caenorhabditis elegans embryos. Mol Biol Cell 13: 4355–4370.
11. Harel A, Forbes DJ (2004) Importin beta: conducting a much larger cellular symphony. Mol Cell 16: 319–330.
12. Rotem A, Gruber R, Shorer H, Shaulov L, Klein E, et al. (2009) Importin beta regulates the seeding of chromatin with initiation sites for nuclear pore assembly. Mol Biol Cell 20: 4031–4042.
13. van der Watt PJ, Maske CP, Hendricks DT, Parker MI, Denny L, et al. (2009) The Karyopherin proteins, Crm1 and Karyopherin beta1, are overexpressed in cervical cancer and are critical for cancer cell survival and proliferation. Int J Cancer 124: 1829–1840.
14. Winnepenninckx V, Lazar V, Michiels S, Dessen P, Stas M, et al. (2006) Gene expression profiling of primary cutaneous melanoma and clinical outcome. J Natl Cancer Inst 98: 472–482.
15. Wang CI, Wang CL, Wang CW, Chen CD, Wu CC, et al. (2011) Importin subunit alpha-2 is identified as a potential biomarker for non-small cell lung cancer by integration of the cancer cell secretome and tissue transcriptome. Int J Cancer 128: 2364–2372.
16. Gluz O, Wild P, Meiler R, Diallo-Danebrock R, Ting E, et al. (2008) Nuclear karyopherin alpha2 expression predicts poor survival in patients with advanced breast cancer irrespective of treatment intensity. Int J Cancer 123: 1433–1438.
17. Mortezavi A, Hermanns T, Seifert HH, Baumgartner MK, Provenzano M, et al. (2011) KPNA2 expression is an independent adverse predictor of biochemical recurrence after radical prostatectomy. Clin Cancer Res 17: 1111–1121.
18. Noetzel E, Rose M, Bornemann J, Gajewski M, Knuchel R, et al. (2012) Nuclear transport receptor karyopherin-alpha2 promotes malignant breast cancer phenotypes in vitro. Oncogene 31: 2101–2114.
19. Tanaka Y, Okamoto K, Teye K, Umata T, Yamagiwa N, et al. (2010) JmjC enzyme KDM2A is a regulator of rRNA transcription in response to starvation. EMBO J 29: 1510–1522.
20. Grummt I (2003) Life on a planet of its own: regulation of RNA polymerase I transcription in the nucleolus. Genes Dev 17: 1691–1702.
21. Murayama A, Ohmori K, Fujimura A, Minami H, Yasuzawa-Tanaka K, et al. (2008) Epigenetic control of rDNA loci in response to intracellular energy status. Cell 133: 627–639.
22. Rigaut G, Shevchenko A, Rutz B, Wilm M, Mann M, et al. (1999) A generic protein purification method for protein complex characterization and proteome exploration. Nat Biotechnol 17: 1030–1032.
23. Nimura K, Ura K, Shiratori H, Ikawa M, Okabe M, et al. (2009) A histone H3 lysine 36 trimethyltransferase links Nkx2–5 to Wolf-Hirschhorn syndrome. Nature 460: 287–291.
24. Shevchenko A, Wilm M, Vorm O, Mann M (1996) Mass spectrometric sequencing of proteins silver-stained polyacrylamide gels. Anal Chem 68: 850–858.
25. Ghoshal K, Majumder S, Datta J, Motiwala T, Bai S, et al. (2004) Role of human ribosomal RNA (rRNA) promoter methylation and of methyl-CpG-binding protein MBD2 in the suppression of rRNA gene expression. J Biol Chem 279: 6783–6793.
26. van der Watt PJ, Ngarande E, Leaner VD (2011) Overexpression of Kpnbeta1 and Kpnalpha2 importin proteins in cancer derives from deregulated E2F activity. PLoS One 6: e27723.
27. Teng SC, Wu KJ, Tseng SF, Wong CW, Kao L (2006) Importin KPNA2, NBS1, DNA repair and tumorigenesis. J Mol Histol 37: 293–299.
28. Moss T (2004) At the crossroads of growth control; making ribosomal RNA. Curr Opin Genet Dev 14: 210–217.
29. Yasuhara N, Shibazaki N, Tanaka S, Nagai M, Kamikawa Y, et al. (2007) Triggering neural differentiation of ES cells by subtype switching of importin-alpha. Nat Cell Biol 9: 72–79.

OPEN

Citation: Cell Death and Disease (2013) 4, e●; doi:10.1038/cddis.2013.234

www.nature.com/cddis

ifn-γ-dependent secretion of IL-10 from Th1 cells and microglia/macrophages contributes to functional recovery after spinal cord injury

H Ishii[1,2,3], S Tanabe[1,2], M Ueno[1,2], T Kubo[3], H Kayama[4,5], S Serada[6], M Fujimoto[6], K Takeda[4,5], T Naka[6] and T Yamashita*[,1,2]

Transfer of type-1 helper T-conditioned (Th1-conditioned) cells promotes functional recovery with enhanced axonal remodeling after spinal cord injury (SCI). This study explored the molecular mechanisms underlying the beneficial effects of pro-inflammatory Th1-conditioned cells after SCI. The effect of Th1-conditioned cells from *interferon-γ* (*ifn-γ*) knockout mice (*ifn-γ* −/− Th1 cells) on the recovery after SCI was reduced. Transfer of Th1-conditioned cells led to the activation of microglia (MG) and macrophages (MΦs), with interleukin 10 (IL-10) upregulation. This upregulation of IL-10 was reduced when *ifn-γ* −/− Th1 cells were transferred. Intrathecal neutralization of IL-10 in the spinal cord attenuated the effects of Th1-conditioned cells. Further, IL-10 is robustly secreted from Th1-conditioned cells in an *ifn-γ*-dependent manner. Th1-conditioned cells from *interleukin 10* knockout (*il*-10 −/−) mice had no effects on recovery from SCI. These findings demonstrate that *ifn-γ*-dependent secretion of IL-10 from Th1 cells, as well as native MG/MΦs, is required for the promotion of motor recovery after SCI.
Cell Death and Disease (2013) **4**, e●; doi:10.1038/cddis.2013.234; published online XX XX 2013
Subject Category: Neuroscience

In mammals, once the central nervous system (CNS) is injured, in contrast to peripheral nervous system, neural regeneration and functional recovery are very limited.[1] Until recently, immune reactions have been considered detrimental after CNS injuries. For example, infiltrating macrophages (MΦs) and resident microglia (MG) are considered deleterious to recovery after CNS injuries[2–4] and T cells are pathogenic in the injured CNS.[4–6] Hence, massive dose of glucocorticoid has been infused to patients after spinal cord injury (SCI) to attenuate immune reactions in the CNS, although there are no convincing evidences that prove significant efficacy of the treatment. However, in some conditions, T cells are beneficial for repair of the injured CNS, although this notion remains controversial.[4,7–9] These contradictory findings regarding the role of T cells after CNS injuries could be explained by differences in the subsets of helper T cells. In support of this hypothesis, a previous study demonstrated that adoptive transfer of interferon-γ (IFN-γ)-producing type-1 helper T-conditioned (Th1-conditioned) cells promote functional recovery after SCI in mice.[10] Enhanced axonal remodeling of corticospinal tract (CST) and serotonergic fibers are also observed in mice that undergo Th1-cell transfer. Although type-2 helper cells (Th2 cells) are considered neuroprotective in some situations,[11,12] this previous study did not demonstrate enhanced recovery from SCI after transfer of Th2-conditioned cells.[10] Furthermore, transfer of IL-17-producing helper T (Th17) cells, pathogenic in multiple sclerosis (MS) and in an animal model of MS,[13] limits recovery in the acute phase after SCI.[10] Importantly, upregulation of the anti-inflammatory/neuroprotective M2 subtype of MG/MΦs was observed in the injured spinal cord after transfer of Th1 cells that had previously been considered to be involved in the onset and progression of autoimmune diseases such as MS.[14,15] In the current study, we explored the mechanism underlying the restorative effects of transferred Th1 cells after SCI in mice.

Results

Therapeutic effects of Th1 cells after SCI depend on IFN-γ. The objective of this study was to explore the mechanism behind the effects of adoptively transferred Th1-conditioned cells on the functional recovery after SCI. We first assessed whether IFN-γ, a major cytokine secreted by Th1 cells,[16] was required for the effects. We isolated cluster of differentiation 4 $(CD4)^+$ T cells from spleens of wild-type

[1]Department of Molecular Neuroscience, Graduate School of Medicine, Osaka University, 2-2 Yamadaoka, Osaka 565-0871, Japan; [2]JST, CREST, 5 Sanbancho, Tokyo 102-0075, Japan; [3]Department of Neurobiology, Graduate School of Medicine, Chiba University, 1-8-1 Inohana, Chiba 260-8677, Japan; [4]Laboratory of Mucosal Immunology, Department of Microbiology and Immunology, Graduate School of Medicine, Osaka University, 2-2 Yamadaoka, Osaka 565-0871, Japan; [5]WPI Immunology Frontier Research Center, Osaka University, 2-2 Yamadaoka, Osaka 565-0871, Japan and [6]Laboratory for Immune Signal, National Institute of Biomedical Innovation, 7-6-8 Saito-Asagi, Osaka 565-0085, Japan
*Corresponding author: T Yamashita, Department of Molecular Neuroscience, Graduate School of Medicine, Osaka University, 2-2 Yamadaoka, Osaka 565-0871, Japan. Tel: +81 66 879 3661; Fax: +81 66 879 3669; E-mail: yamashita@molneu.med.osaka-u.ac.jp
Keywords: Th1 cells; spinal cord injury; microglia macrophages; interleukin 10
Abbreviations: CNS, central nervous system; CST, corticospinal tract; SCI, spinal cord injury; IFN-γ, interferon-γ; IL-10, interleukin 10; Th1 cells, type-1 helper T cells; Th2 cells, type-2 helper T cells; Th17, IL-17-producing helper T cells; NT-3, neurotrophin 3; CD4, cluster of differentiation 4; PBS, phosphate-buffered saline; GDNF, glia-derived neurotrophic factor; ELISA, enzyme-linked immunosorbent assay
Received 28.10.12; revised 06.5.13; accepted 03.6.13; Edited by A Verkhratsky

(WT) and *interferon-γ* (*ifn-γ*)-knockout (*ifn-γ* −/−) mice. The cells were then cultured with IL-2/IL-12 and anti-IL-4 neutralizing antibody to induce differentiation into Th1 cells. We confirmed with enzyme-linked immunosorbent assay (ELISA) that IFN-γ secretion from Th1 *ifn-γ* −/− cells was totally abrogated compared with WT Th1 cells and Th17 cells (Figure 1a). In addition, abundant expression of T-bet, a T-box transcription factor of the Th1 master gene,[17] was observed in cultured WT Th1-conditioned cells by flow cytometry (Figure 1b). T-bet in *ifn-γ* −/− Th1-conditioned cells was expressed at an intermediate level between Th0 and Th1 cells (Figure 1b).

Mouse vertebrae were laminectomized and the exposed spinal cords were contused at the level between thoracic vertebrae 9 (T9) and 10 (T10) by an impactor with a force of 60 kdyn. On the first day after contusion, the hindlimbs of all mice were completely paraplegic and gradually displayed partial recovery of motor function after day 1. At 4 days after contusion SCI, 1.0×10^7 WT and *ifn-γ* −/− Th1-conditioned cells were transferred intraperitoneally (i.p.) into the mice and recovery of motor function was assessed using the Basso Mouse Scale (BMS).[18] Enhanced motor recovery was observed in mice that received Th1 *ifn-γ* −/− cell transfer compared with control mice, but the extent of the improvement was less than that observed in mice receiving a transfer of WT Th1-conditioned cells (Figure 1c).

Consistent results were obtained when the grid-walk test was performed, which assesses voluntary movement control mediated by the corticospinal and the rubrospinal systems.[19] Transfer of Th1 *ifn-γ* −/− cells led to a significantly greater frequency of hindlimb dropping (mistakes) compared with that of WT Th1 cells (Figure 1d). Thus, IFN-γ in Th1-conditioned cells contributes to improved functional recovery.

***ifn-γ*-dependent activation of MG by adoptive transfer of Th1-conditioned cells.** Previous observations with flow cytometry after SCI showed that transfer of Th1-conditioned cells led to an increase in MG/MΦs and to upregulation of the neuroprotective M2 subtype: $CD206^+$ cells among the MΦs and arginase 1^+ (Arg1) cells among the MG.[10] Morphological analysis by immunohistochemistry for ionized calcium-binding adapter molecule 1 (Iba1) in the contused spinal cord revealed that with Th1 transfer, MG/MΦs increased, enlarged, and were more round compared with those in control mice (Figures 2a and b). This observation is consistent with the previous data that showed both activation of MG/MΦs with CD11b and CD45 immunoreactivity using flow cytometry and upregulation of the M2 subtype, which has characteristics including anti-inflammatory effects, phagocytic behavior, and a round shape compared with the pro-inflammatory, destructive, and ramified M1 subtype.[10] MG/MΦs were assessed quantitatively using flow cytometry[20] and microglial activation by Th1-cell transfer after SCI was shown to depend on IFN-γ (Figures 2c and d).

IL-10 produced from MG/MΦs contributes to repair after SCI. It was hypothesized that some molecules secreted from

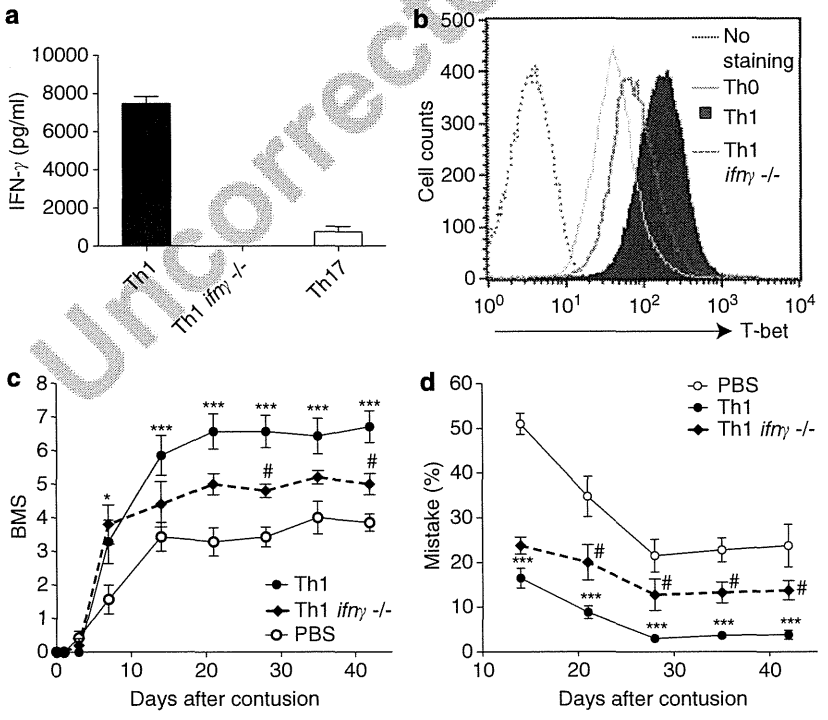

Figure 1 Improved recovery induced by Th1 cells after SCI depends on IFN-γ. Enhanced recovery from SCI by Th1 transfer is dependent on *interferon-γ* (*ifn-γ*) in transferred Th1 cells. (**a**) Level of IFN-γ secreted from Th1 cells, Th1 *ifn-γ* −/− cells, and Th17 cells, which was detected by ELISA($n=3$). (**b**) Comparison of T-bet production in helper T cells differentiated *ex vivo*, which was assessed by flow cytometry histogram. Representative data from three independent experiments. (**c**) Time course of hindlimb locomotion using the BMS with adoptive transfer of 1.0×10^7 each helper T-cell subsets (PBS, $n=7$; Th1 $n=7$; Th1 *ifn-γ* −/−, $n=5$). (**d**) Time course of the grid-walk test (PBS, $n=4$; Th1, $n=6$; Th1 *ifn-γ* −/−, $n=4$). Data are presented as mean ± S.E.M. $^{**}P<0.01$, $^{***}P<0.001$ versus the PBS group, $^{\#}P<0.05$ *versus* Th1 group (two-way ANOVA with repeated measures, Bonferroni post-test)

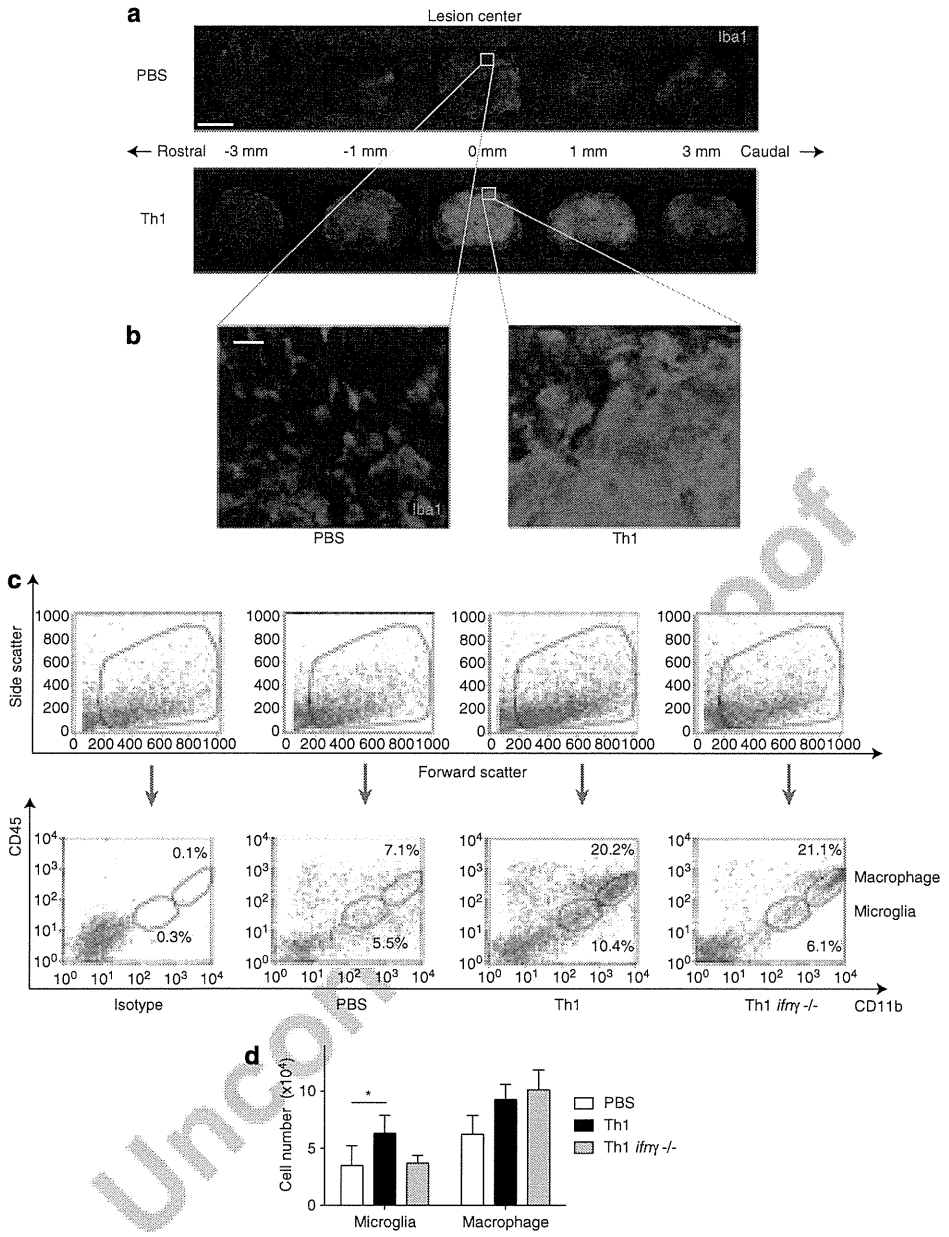

Figure 2 Microglial activation induced by Th1-cell transfer depends on IFN-γ. Adoptive transfer of Th1-conditioned cells after SCI leads to activation of MG/MΦs at the injured site, and microglial activation is dependent on *ifn-γ* in transferred Th1 cells. (**a**) Immunohistochemistry for MG/MΦs labeled with anti-Iba1 antibody. Spinal cords removed on day 10 after SCI were cut transversely. The section at 0 mm corresponds to the epicenter of the contusion and the distance shown is caudal from the epicenter. Scale bar, 500 μm. (**b**) Higher magnification views of (**a**). Scale bar, 100 μm. (**c**) Representative flow cytometry profile of MG/MΦs that accumulated in the spinal cord on SCI day 6, 2 days after the injection of PBS or cultured T cells. Upper dot plots indicate the side-scatter/forward-scatter profile by which CD11b/CD45 profiles were gated. In lower dot plots, CD11b ^{intermediate} CD45 ^{intermediate} corresponds to MG, whereas CD11b ^{high} CD45 ^{high} corresponds to MΦs. The leftmost dot plots indicate a profile using isotype-matched immunoglobulins as a control. (**d**) The number of MG or MΦs that accumulated in the spinal cord on day 6 after SCI, 2 days after the injection of PBS or Th1-conditioned cells. PBS, $n=3$; Th1, $n=4$; Th1 *ifn-γ* $-/-$, $n=3$. Leukocytes isolated from the spinal cords of two to four mice were analyzed in each experiment. $^*P<0.05$ (one-way ANOVA with Bonferroni post-test)

MG/MΦs have a role in the enhanced functional recovery induced by Th1-cell transfer after SCI. Intracellular cytokine staining of MG/MΦs indicated that interleukin 10 (IL-10), which is considered to be cerebroprotective after an ischemic stroke[21] and is one of the M2 anti-inflammatory markers,[22] was upregulated in MG/MΦs in the spinal cord after transfer of Th1-conditioned cells (Figure 3a). This upregulation was reduced if Th1 *ifn-γ* $-/-$ cells were adoptively transferred (Figure 3a), demonstrating that IFN-γ secreted from Th1-conditioned cells contributes to IL-10 production from MG/MΦs. We previously demonstrated that neutralization of IL-10 from Th1 cells attenuates the functional recovery initiated by the transfer of Th1 cells after SCI.[10] However, it remains to be determined whether IL-10 secretion in the CNS

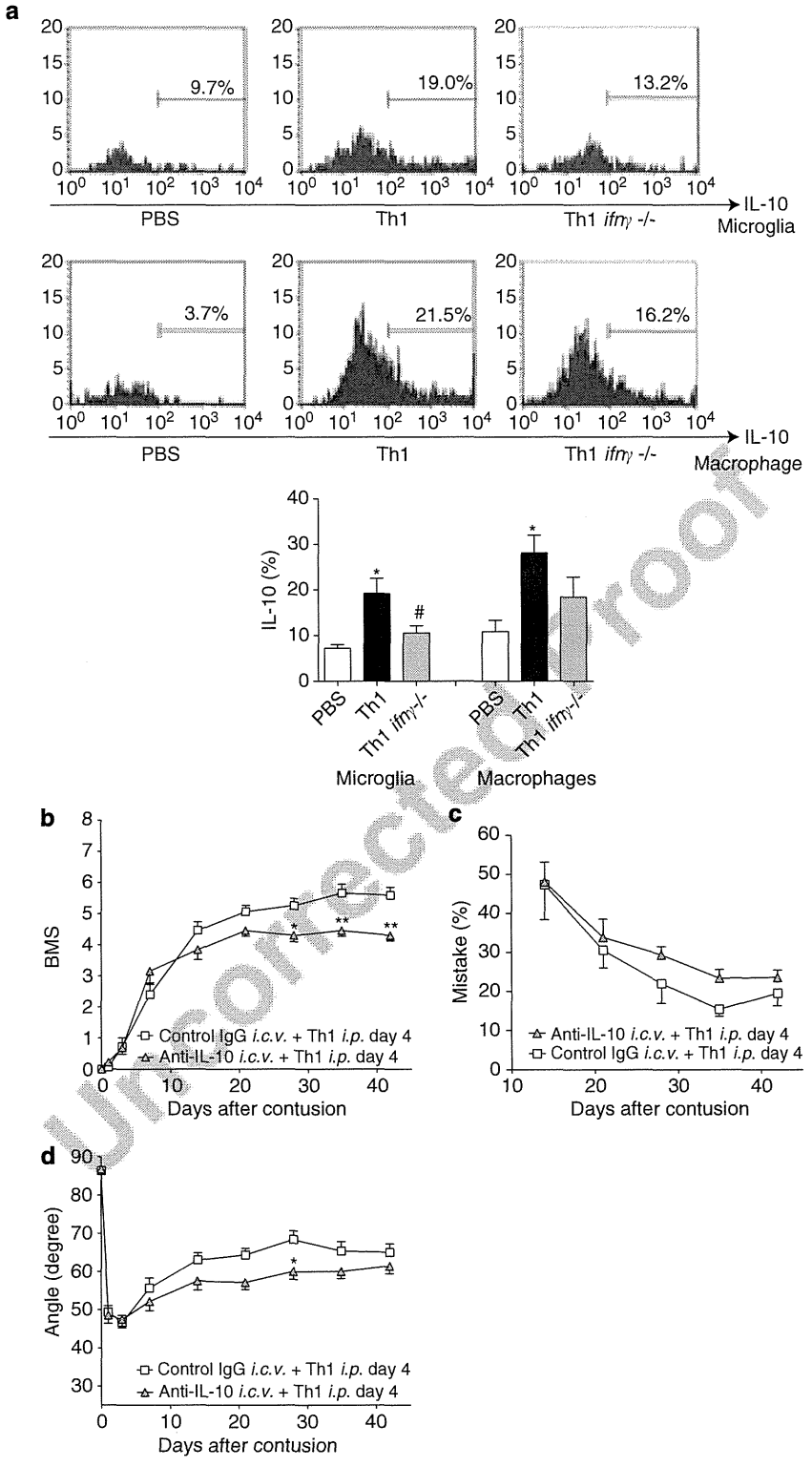

Figure 3 Neutralization of IL-10 in the CNS attenuates functional recovery by Th1 cells transfer. IL-10 expressed in the CNS partially contributes to functional recovery after SCI with adoptive transfer of Th1-conditioned cells. (**a**) Upper histograms: comparison of IL-10 production from MG/MΦs evaluated using histograms of intracellular cytokine staining. The histogram is representative of four independent experiments. All histograms were gated from the populations of MG or MΦs as shown in Figure 2c. Lower graph: quantification of IL-10 production as indicated above. $^{*}P<0.05$ *versus* the PBS group, $^{\#}P<0.05$ *versus* Th1 group (one-way ANOVA, Bonferroni post-test). (**b–d**) Functional recovery from SCI evaluated by: BMS scores (**b**), grid-walk test (**c**), and inclined-plane test (**d**) in Th1-conditioned cell-transferred SCI mice treated with control IgG or anti-IL-10 antibody into the cerebral ventricles (i.c.v.; control rat IgG + Th1, $n=15$; anti-IL-10 + Th1, $n=13$ (BMS scores and inclined-plane test)/control IgG + Th1, $n=9$; anti-IL-10 + Th1, $n=8$ (grid-walk test)). $^{*}P<0.05$ *versus* control IgG + Th1 group (two-way ANOVA with repeated measures, Bonferroni post-test)

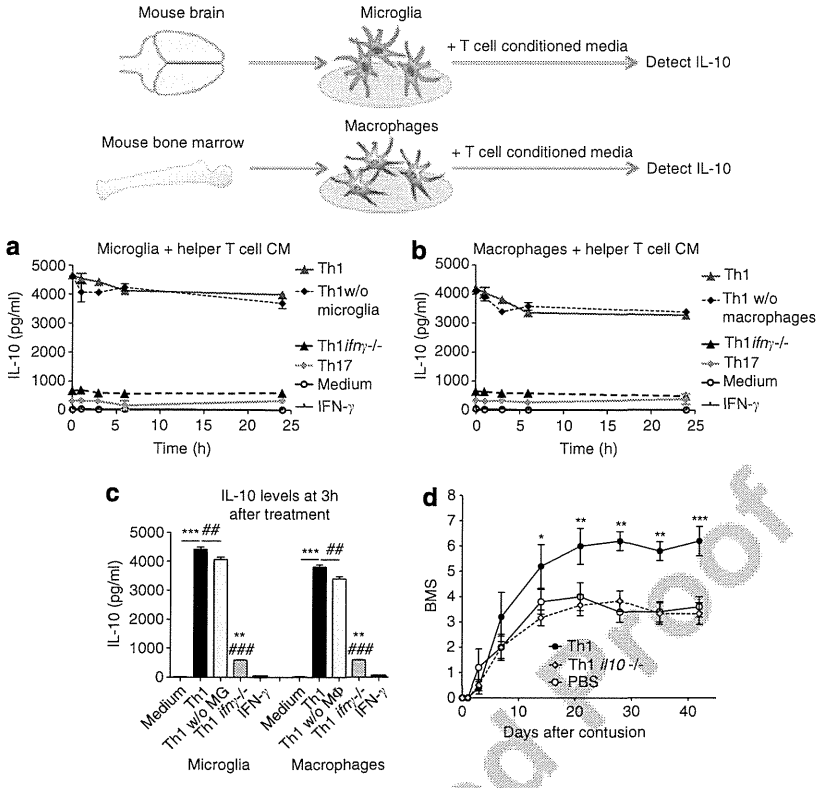

Figure 4 *In vitro* assay for IL-10 detection in MG/MΦ culture and *in vivo* experiment using *il*-10-knockout mice. Neonatal mouse brain-derived MG or mouse femoral bone marrow-derived MΦs were cultured on 96-well plate. The MG or the MΦs were treated with the T-cell conditioned media (CM) or recombinant IFN-γ and, thereafter, IL-10 levels at different time points were measured by using ELISA (schematic drawn in an upper panel). IL-10 surge from MG/MΦs was not observed in the *in vitro* assay unlike in the injured spinal cord after Th1-cell transfer. However, Th1 cells secreted robust IL-10 in an *ifn-γ*-dependent manner, and this IL-10 secretion from Th1 cells had a pivotal role in improved recovery after SCI. (**a**) Time course of IL-10 level detected by ELISA in MG culture media after treatment with T-cell CM or IFN-γ (medium, $n=4$; Th1, $n=4$; Th1 w/o MG: Th1 cells without MG, $n=4$; Th1 *ifn-γ* −/−, $n=3$; IFN-γ (recombinant IFN-γ at 20 ng/ml), $n=3$; Th17, $n=2$). (**b**) Time course of IL-10 level detected by ELISA in macrophage (MΦ) culture media after treatment with T-cell CM or IFN-γ (medium, $n=4$; Th1, $n=4$; Th1 w/o microglia (MG): Th1 cells without MΦs, $n=4$; Th1 *ifn-γ* −/−, $n=3$; IFN-γ: recombinant IFN-γ at 20 ng/ml, $n=3$; Th17, $n=2$). (**c**) IL-10 level in MG or MΦ culture media at 3 h after treatment with T-cell CM or IFN-γ (MG: medium, $n=4$; Th1, $n=4$; Th1 cells without MG, $n=4$; Th1 *ifn-γ* −/−, $n=3$; IFN-γ: recombinant IFN-γ at 20 ng/ml, $n=3$; MΦs: medium, $n=4$; Th1, $n=4$; Th1 w/o MΦ: Th1 cells without MG, $n=4$; Th1 *ifn-γ* −/−, $n=3$; IFN-γ: recombinant IFN-γ at 20 ng/ml, $n=3$). $^{**}P<0.01$, $^{***}P<0.001$ *versus* the medium group, $^{\#\#}P<0.01$, $^{\#\#\#}P<0.001$ *versus* Th1 group (one-way ANOVA, Bonferroni post-test). (**d**) BMS scores in Th1 or Th1 *il*-10 −/− -transferred SCI mice (PBS, $n=5$; Th1, $n=5$; Th1 *il-10* −/−, $n=6$). $^{*}P<0.05$, $^{**}P<0.01$, $^{***}P<0.001$ *versus* the PBS group (two-way ANOVA with repeated measures, Bonferroni post-test)

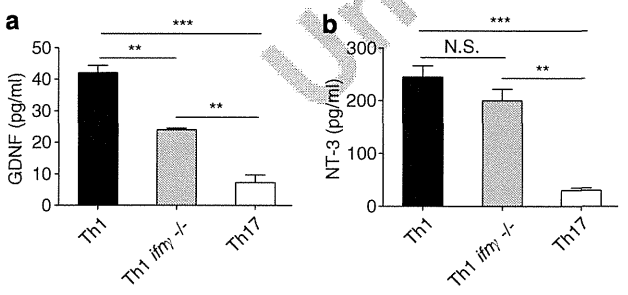

Figure 5 GDNF secretion from Th1 cells is dependent on IFN-γ. Expression of neurotrophic factors in cultured helper T cells. GDNF (**a**), and NT-3 (**b**) in the supernatant of Th1, Th1 *ifn-γ* −/−, and Th17 cells detected by ELISA (Th1, $n=3$; Th1 *ifn-γ* −/−, $n=3$; Th17, $n=3$). $^{**}P<0.01$, $^{***}P<0.001$; NS, not significant (one-way ANOVA with Bonferroni post-test)

after Th1 transfer has neuroprotective effects, because anti-IL-10-neutralizing antibody could block not only IL-10 secretion from transferred Th1 cells but also from native cells in the injured CNS, as shown in our previous experiment. To assess whether IL-10 produced by MG/MΦs in the CNS is required for the *in vivo* effects, anti-IL-10-neutralizing antibody or control IgG was injected into the cerebral ventricles (i.c.v.) using an osmotic pump catheterized to the right lateral ventricle for 7 days after SCI in mice. Th1-conditioned lymphocytes were injected i.p. to these mice on day 4 after SCI. Compared with treatment with control IgG, antibody infusion significantly suppressed motor recovery at time points later than 4 weeks after SCI, as assessed by BMS scoring (Figure 3b). Although there were no significant differences observed in the grid-walk test (Figure 3c), the ameliorated recovery of motor functions by Th1-cell transfer was attenuated in the inclined-plane test (Figure 3d). Therefore, IL-10 secreted from the cells in the CNS is a partial contributor to enhanced motor recovery after SCI.

***ifn-γ*-dependent secretion of IL-10 from Th1 cells have a pivotal role in improved recovery after SCI.** We next performed *in vitro* experiments to confirm whether we can recapitulate IL-10 upregulation from MG and MΦs by Th1-

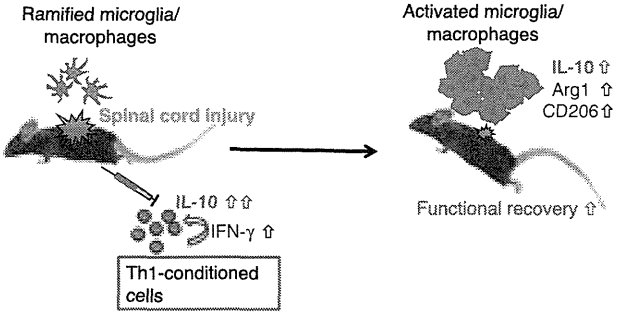

Figure 6 Schematic representation showing molecular mechanism of restorative effects of transferred Th1-conditioned lymphocytes on recovery after SCI. *ifn-γ-dependent secretion of IL-10 from transferred Th1-conditioned cells* contributes to an increase of M2 subtype of MG/MΦs, as shown by the upregulation of IL-10, arginase 1 (Arg1), and CD206, leading to restorative effects on functional recovery after SCI

conditioned lymphocytes. First, we cultured MG from neonatal mouse brains and mouse femoral bone-derived MΦs. Secretion of IL-10 was measured using ELISA after MG (Figure 4a), or MΦs (Figure 4b) cultured in 96-well plates were treated with conditioned media (CM) of Th1 cells, Th1 *ifn-γ −/−* cells, and Th17 cells or recombinant IFN-γ (Figure 4 upper schematic). Even at the starting point, high levels of IL-10 were observed in Th1-cell group (Figures 4a and b), demonstrating that CM of Th1 cells themselves contained abundant IL-10 compared with Th1 *ifn-γ −/−* cells and Th17 cells. Although IL-10 expression from MG/MΦs unexpectedly did not surge, IL-10 levels from MG or MΦs treated with CM of Th1 cells were significantly higher than only CM of Th1 cells at 3 h after the treatment (Figures 4a–c). It is suggested that comparatively small amounts of IL-10 were secreted from cultured MG/MΦs in the early phase after treatment of Th1 CM. As Th1 cells robustly secreted neuroprotective IL-10 (Figures 4a and b), we examined whether genetic deletion of *il*-10 in transferred Th1-conditioned cells decreased the effects of the Th1 cells in SCI mice. As a result, Th1 interleukin 10 knockout (*il-10 −/−*) cells transfer completely diminished the ameliorative effects of Th1 cells transfer on hindlimb locomotion after SCI, as assessed by BMS scoring (Figure 4d).

Th1-conditioned lymphocytes secrete neurotrophic factors. Candidate neurotrophic factors in Th1-conditioned cells that promote neuroprotection were investigated after contusion SCI and the expression of neurotrophic factors, such as glia-derived neurotrophic factor (GDNF) and neurotrophin 3 (NT-3), in Th1-conditioned cells was shown to be higher than that in Th17 cells, which limited functional recovery after SCI.[10] It has been shown that GDNF is neuroprotective after SCI[23] and that NT-3 promotes growth and differentiation of neurons and synapses.[24] In the current study, the expression levels of GDNF and NT-3 among Th1 cells, Th1 *ifn-γ −/−* cells, and Th17 cells were compared using ELISA. GDNF expression was higher in Th1 cells than that in Th1 *ifn-γ −/−* cells or Th17 cells (Figure 5a), although expression of NT-3 was not significantly different between Th1 cells and Th1 *ifn-γ −/−* cells (Figure 5b).

Discussion

The current study demonstrated that *ifn-γ*-dependent secretion of IL-10 from Th1 cells as well as from MG/MΦs is required for the enhanced recovery from SCI induced by Th1 transfer (Figure 6). It is surprising that expression of the neuroprotective cytokine IL-10 is upregulated from MG/MΦs in an *ifn-γ*-dependent manner (Figure 3a), although pro-inflammatory Th1 cells were transferred after SCI. However, effects of these cytokines especially IL-10 upregulation in the CNS are partial (Figures 3b and d). Th1 cell-transferred spinal cord after SCI showed accumulation of activated round MG and MΦs around the injured dorsal and lateral CST, although activated and ramified MG/MΦs are also observed without treatment after SCI (Figures 2a and b). It is suggested that the increased proportion of neuroprotective M2 MG/MΦs induced by Th1 cells transfer[10] may protect and repair injured neuronal fibers, including the CST. To elucidate the progression of IFN-γ from Th1 cells leading to IL-10 upregulation in MG/MΦs, we treated cultured MG/MΦs with Th1 CM or recombinant IFN-γ and measured IL-10 levels (Figures 4a–c). The result suggests that Th1 cells themselves secrete abundant IL-10 and, comparatively, an unexpectedly small amount of IL-10 was secreted from MG/MΦs when treated with Th1 CM. It is possible that the cell state of the cultured MG/MΦs in our system may be different from *in vivo* MG/MΦs after SCI (Figure 3a) and that other micro-environmental factors, such as astrocyte activity, may be required to robustly elevate IL-10 secretion from MG/MΦs. Whereas experiments neutralizing IL-10 in the CNS only attenuated the effects of Th1-conditioned cells transfer (Figures 3b and d), transfer of Th1-conditioned cells derived from *il*-10 −/− mice showed complete abrogation of the restorative effects of Th1 cells (Figure 4d). Thus, *ifn-γ*-dependent secretion of IL-10 from transferred Th1 cells (Figures 4a and b) may contribute to the entirety of the effects by directly shifting the CNS into a neuroprotective state[25] in addition to increasing the proportion of the neuroprotective M2 subtype of MG/MΦs observed and upregulation of Arg1, CD206,[10] and IL-10 (Figure 6). Indeed, transfer of Th1-conditioned cells has enhanced restorative effects compared with just inducing viral expression of IL-10 in the CNS after SCI.[25] This may be caused by shifting systems in the periphery, such as MΦs in the lymph nodes into a neuroprotective state, as well as the CNS with Th1-cell transfer. On the other hand, IFN-γ did not have direct effects on IL-10 upregulation from MG/MΦs (Figures 4a–c). We conclude that *ifn-γ* is required to maintain transferred Th1 cells to abundantly secrete IL-10 rather than directly upregulating IL-10 from MG/MΦs in the lesion site after SCI. Our result is consistent with a report that *ifn-γ* mediates IL-10 reactivation by parasite-reactive Th1 cells.[26] The notion may be consistent with our previous report that IFN-γ is necessary for maintaining Th1 cells to promote neurite outgrowth from cortical neurons rather than directly elongating neurites.[27] On the other hand, other mechanism independent of *ifn-γ* may be partially responsible for IL-10 secretion from Th1 cells, because comparatively very small amounts of IL-10 were still secreted from Th1 *ifnγ −/−* cells (Figures 4a and b). This residual secretion of IL-10 may be attributed to *ifn-γ*-independent activation of signal transducer and activator of transcription 4, as previously reported.[28]

In general, inflammation is considered to be detrimental to the CNS injury, but there are some reports demonstrating that pro-inflammatory T cells are beneficial to the CNS injury. Those T cells may be attributed to the functions of Th1 cells in *ifn-γ*-dependent manner. Indeed, IFN-γ promotes neuronal differentiation[29] and neurogenesis.[30] Secretion of IFN-γ by the transferred Th1-conditioned cells has a role in MG activation (Figures 2c and d), leading to functional recovery from SCI. It has been suggested that activated MG induce neuronal differentiation[31] and are neuroprotective.[22] In addition, the beneficial role of MΦs in the injured CNS is known.[32,33]

IFN-γ contributes to the upregulation of GDNF in Th1 cells (Figure 5a), which may have positive effects on neuroprotection after SCI. Thus, the *in vivo* effects of IFN-γ secreted by Th1-conditioned cells are important for functional recovery after SCI. However, it should be noted that Th1-conditioned cells lacking IFN-γ still had limited beneficial effects (Figures 1c and d). These remnant effects may be mediated by neuroprotective IL-10 (Figures 4a and b) and trophic factors, such as NT-3 (Figure 5b).

Taken together, pro-inflammatory Th1 cells have restorative effects on functional recovery after SCI in *ifn-γ*- and *il-10*-dependent manner. There are many side effects after massive dose of glucocorticoid treatment such as increased susceptibility to infection, gastroinstestinal ulcer, diabetes mellitus, and mental disorder. Therefore, our study provides new insights into future immunomodulatory treatment after CNS trauma (for example, transfer of Th1 cells or skewing to Th1), which not only promotes beneficial immune reactions but also attenuates harmful ones such as devastating Th17 cells.

Materials and Methods

Mice. C57BL/6j mice were purchased from Charles River Laboratories (Wilmington, MA, USA). As previously reported, *ifn-γ* −/− mice[34] and *il-10* −/− mice[35] on the C57BL/6 background were used. All mice used in this study were housed in specific pathogen-free conditions and were treated and cared for in accordance with the guidelines of Osaka University pertaining to the treatment of experimental animals.

Animal model of SCI. Adult (7–9 weeks old) female C57BL/6 mice were anesthetized with sodium pentobarbital (50 mg/kg; Kyoritsu Seiyaku, Tokyo, Japan). Following dorsal laminectomy (at the T9–T10 level), the spinal cord was contused with a force of 60 kdyn using an Infinite Horizon Impactor (Precision Systems & Instrumentation, Fairfax Station, VA, USA), as previously described.[36] The muscle and skin layers were then sutured. The bladder was expressed daily using manual abdominal pressure until 10 days after injury. Food and water were provided *ad libitum*.

Adoptive transfer of cultured T cells. The procedure was performed according to a previously described procedure.[10] The procedure is briefly indicated as following: spleens were collected from the mice. $CD4^+$ T cells were isolated using magnet sorting with anti-CD4 magnet beads (Miltenyi Biotec, Cologne, Germany). $CD4^+$ T cells were stimulated with anti-CD3-ε/anti-CD28 antibodies (5 μg/ml, respectively, Pharmingen/BD Biosciences) coated on 24-well plates (Greiner Bio-One, Kremsmünster, Austria). Th1-conditioned cells were differentiated by the addition of recombinant IL-2 (25 U/ml; R&D Systems/TECHNE, Minneapolis, MN, USA), IL-12 (10 U/ml; R&D systems), and anti-IL-4 antibodies (25% culture supernatant of hybridoma; clone HB-188; American Type Culture Collection, Manassas, VA, USA). Th17-conditioned cells were differentiated by the addition of recombinant IL-6 (20 ng/ml; R&D systems), IL-23 (20 ng/ml; R&D systems), TGF-β1 (3 ng/ml; R&D systems), anti-IL-4 antibodies (25% culture supernatant of the hybridoma), and anti-IFN-γ antibodies (1% culture supernatant of hybridoma; clone HB-170; American Type Culture Collection) in the presence of anti-IL-2 antibody (10 μg/ml; R&D Systems). Th0 cells were cultured in the presence of only IL-2 (25 U/ml; R&D Systems). On day 4, the helper T cells were collected. The cells were centrifuged at 1000 × *g* for 20 min with Lympholyte-M (Cedarlane Laboratories, Burlington, Ontario, Canada), and the intermediate layer was collected to eliminate the dead cells. The cells were restimulated for 3 h with anti-CD3-ε and anti-CD28 antibodies. On day 4 after SCI, helper T cells (1.0×10^7) suspended in 500 μl phosphate-buffered saline (PBS) were injected i.p. into mice. As a control, 500 μl PBS was injected into mice after SCI.

Behavioral analysis. Hindlimb motor function was evaluated using the BMS open-field locomotor test, in which scores range from 0 to 9.[18] BMS scores were recorded on days 1, 3, and 7 after injury, and once weekly thereafter for a total of 6 weeks.

The grid-walk test was also performed to evaluate hindlimb locomotion.[19] Deficits in descending motor control were examined by assessing the ability of mice to step on a square framework, 26 cm on a side, consisting of 1-cm^2 grids made of round metal bars. Analysis was performed by counting the number of errors (that is, dropping the hindlimb from the grid) in 50 steps for each hindlimb. The mean percentage of errors was then calculated. Error percentages were not calculated before 2 weeks after SCI because, before this time, animals were unable to move their hindlimbs owing to insufficient recovery.

A subset of animals was analyzed using the inclined-plane test,[10] which evaluates the animal's ability to maintain body position on a board raised incrementally to increasing angles. Performance on the inclined plane correlates with the integrity of the rubrospinal tract (and other nonpyramidal pathways) after SCI. Animals were tested at days 1, 3, 7 after injury, and once weekly thereafter for a total of 6 weeks. Mice were tested in each position, after which the angle was increased incrementally by 5°. The maximum angle at which the animal could maintain a stationary position on the board for 10 s was recorded. Investigators were blinded to the treatment protocol and recorded behavioral scores.

Tissue preparation and histochemistry. For histochemistry, animals were perfused with 4% paraformaldehyde and preserved spinal cord tissues were collected. The entire spine was dissected out and post-fixed in 4% paraformaldehyde for 3 h at 4 °C. The spinal cord was removed from the vertebral column and stored for 12 h in 15% sucrose in 0.2 M PBS at 4 °C. The spinal cord was then placed in 30% sucrose in 0.2 M PBS for 24 h at 4 °C. The spinal cord was embedded in Tissue Tek OCT compound (Sakura, Tokyo, Japan) and immediately frozen on dry ice at − 80 °C. A series of 20-μm transverse sections were cut on a cryostat and mounted on Matsunami Adhesive Silan-coated glass slides (Matsunami Glass, Osaka, Japan). After washing three times with PBS, all sections were blocked in PBS containing 5% BSA and 0.3% Triton X-100 for 1 h at room temperature. The sections were then incubated with polyclonal anti-Iba1 antibody (1 : 200; Wako, Osaka, Japan) overnight at 4 °C, washed three times with PBS, and incubated with fluorescein-conjugated secondary antibodies (1 : 500; Life Technologies, Carlsbad, CA, USA) for 1 h at room temperature. Sections were then rinsed three times in PBS and mounted. The sections were viewed under an inverted light microscope equipped with epifluorescence optics and a dry condenser for phase-contrast microscopy (DP70, Olympus, Tokyo, Japan).

Preparation of leukocytes from injured spinal cords. The extraction of leukocytes from the spinal cord was performed according to a previously described procedure.[37] First, mice were transcardially perfused with ice-cold PBS. The spinal cord was then dissected and suspended in Hank's Balanced Salt Solution (Life Technologies) supplemented with 3% fetal bovine serum (FBS), 100 IU/ml penicillin, and 100 μg/ml streptomycin. The spinal cords were digested with collagenase D (5.0 mg/ml; Roche Diagnostics, Tokyo, Japan) plus 2.5 mM calcium chloride. After filtration with a 70-μm Cell Strainer (BD Biosciences), lysis of red blood cells with RBC Lysis Buffer (BioLegend, San Diego, CA, USA) and washing, the pellet, isolated by 38% Percoll centrifugation at 1500 × *g* for 20 min, was collected for flow cytometry.

Cell-surface and intracellular antigen staining. Cultured lymphocytes or collected leukocytes from mouse spinal cords were stimulated with 50 ng/ml phorbol 12-myristate 13-acetate (Sigma-Aldrich, St. Louis, MO, USA) and 750 ng/ml ionomycin (Calbiochem/EMD Millipore, Billerica, MA, USA) for 4 h and with 10 μg/ml brefeldin A (Sigma-Aldrich) for the last 2 h. The cells were suspended in Fixation Buffer (eBioscience, San Diego, CA, USA) and surface stained with anti-CD45-Alexa647 (BioLegend) and anti-CD11b-PE (BioLegend).

Intracellular staining was performed according to the manufacturer's protocol, using anti-T-bet-PE (eBioscience) and anti-IL-10-FITC (BioLegend).

Flow cytometric analysis. Flow cytometry was performed with the FACSCalibur flow cytometer (BD Biosciences), and was analyzed using ProQuest (BD Biosciences) and FlowJo software (TreeStar, Ashland, OR, USA). Control experiments using isotype-matched immunoglobulins (BioLegend) were performed to determine the specificity of the signals of antibodies against specific antigens.

Infusion i.c.v. Following SCI, the right lateral ventricle of the mouse was stereotaxically perforated with a brain infusion kit 3 (ALZET, DURET Corporation, Cupertino, CA, USA; coordinates: 0.5 mm posterior to the bregma, 1.0 mm lateral to the bregma, 2 mm deep) and connected to an osmotic minipump (ALZET; pump model: 1007D) filled with 1 mg/ml anti-IL-10-neutralizing antibody (eBioscience; clone: JES5-16E3) or rat IgG (eBioscience). The anti-IL-10 antibody was infused for 7 days.

Culture of MG/MΦs and treatment of T-cell culture media. Culture of MG and MΦs was performed according to a previously described procedure.[38] MG were obtained from the brain of C57BL/6j mice on postnatal day 1–2. The cerebral cortex of each mouse was dissected out and the meninges were eliminated. The brains were minced with surgical knives, and then digested with 0.25% trypsin for 15 min and 0.5 mg/ml DNase for the last 1 min at 37 °C. The cells were passed through a 70-μm Cell Strainer (BD Biosciences). The resultant cell suspension was diluted with Dulbecco's Modified Eagle Medium (DMEM; Invitrogen) and spun down. The pellet was suspended with 10% FBS/1% penicillin and streptomycin/DMEM (DMEM growth medium) and plated on poly-L-lysine-coated 75-cm^3 culture flask (Greiner Bio-One). On day 1 and every 3 days thereafter, DMEM growth medium was replaced. After >7 days, the flask was shaken for 30 min so that floating MG could be collected from the astrocyte monolayer sheet and cultured at the density of 3.3×10^4 cells in 100 μl growth medium for 1 well of 96-well plate (Greiner Bio-One). More than 90% of the cells were CD11b$^+$ MG.

Bone marrow-derived MΦs were obtained from bilateral femoral bones of 9-week-old C57BL6/j mice. Marrow cores were flushed using 10-ml syringes filled with RPMI1640 (Invitrogen)/10% FBS. After trituration and lysis of red blood cells with RBC Lysis Buffer (BioLegend), the cells were washed in the medium, and then plated and cultured in RPMI1640 with 10% FBS, penicillin/streptomycin (RPMI growth medium), and M-CSF (50 ng/ml; BioLegend). Non-adherent cells were collected at day 4. On day 6, the cells were replated on 96-well plates at the density of 3.3×10^4 cells in 100 μl of RPMI growth medium for one well. On day 7, the cells were treated with the T-cell supernatant. More than 90% of the cells were CD11b$^+$ MΦs.

One hundred microliters of CM of cultured T cells (collected 4 days after T-cell culture) or 40 ng/ml IFN-γ (BioLegend) dissolved in 100 μl medium were applied to MG or MΦs cultured as above. At 0, 1, 3, 6, and 24 h after treatment of T-cell CM, supernatant of the cultured cells were collected to detect IL-10 with ELISA.

Enzyme-linked immunosorbent assay. Th1, Th1 *ifn-γ −/−*, and Th17 cells were prepared as described above. Three hours after restimulation with anti-CD3-ε/anti-CD28 antibodies, cells were centrifuged and their supernatants were collected and stored at −80 °C until use. Concentrations of IFN-γ, IL-10, NT-3, and GDNF in the supernatants of each cell were analyzed using the ELISA kits, according to the manufacturer's protocol (IFN-γ and IL-10: R&D Systems; NT-3: Emax Immunoassay System; GDNF: Promega, Fitchburg, WI, USA). Absorbance values were read at 450 nm on a plate reader (SpectraMax M2; Molecular Devices, Sunnyvale, CA, USA).

Statistical analysis. All values are expressed as mean ± S.E.M. Motor function scores were analyzed using two-way ANOVA with repeated measures with a Bonferroni post-test for 2–3 groups. For all other data, a one-way ANOVA with a Bonferroni post-test collection was used. Values of $P<0.05$ were considered statistically significant.

Conflict of Interest

The authors declare no conflict of interest.

Acknowledgements. We thank Drs. T Nakayama, M Yamashita, and M Kuwahara at Chiba University for their technical advice on T-cell culture; Drs. K Morimoto and S Lee at Osaka University for their help in histological assessment; Ms Nakamura at Osaka University for her advise on surgical procedure; Dr. Y Souma at the National Institute of Biomedical Innovation for taking care of the IFN-γ knockout mice; and Drs. H Iijima, A Mukai, H at Osaka University for advice on knockout mice. This work was supported by a research grant from a Grant-in-Aid for Young Scientists (S) from the Japan Society for the Promotion of Science (JSPS).

1. David S, Aguayo AJ. Axonal elongation into peripheral nervous system 'bridges' after central nervous system injury in adult rats. *Science* 1981; **214**: 931–933.
2. Bye N, Habgood MD, Callaway JK, Malakooti N, Potter A, Kossmann T *et al.* Transient neuroprotection by minocycline following traumatic brain injury is associated with attenuated microglial activation but no changes in cell apoptosis or neutrophil infiltration. *Exp Neurol* 2007; **204**: 220–233.
3. Beck KD, Nguyen HX, Galvan MD, Salazar DL, Woodruff TM, Anderson AJ. Quantitative analysis of cellular inflammation after traumatic spinal cord injury: evidence for a multiphasic inflammatory response in the acute to chronic environment. *Brain* 2010; **133**: 433–447.
4. Donnelly DJ, Popovich PG. Inflammation and its role in neuroprotection, axonal regeneration and functional recovery after spinal cord injury. *Exp Neurol* 2008; **209**: 378–388.
5. Potas JR, Zheng Y, Moussa C, Venn M, Gorrie CA, Deng C *et al.* Augmented locomotor recovery after spinal cord injury in the athymic nude rat. *J Neurotrauma* 2006; **23**: 660–673.
6. Shichita T, Sugiyama Y, Ooboshi H, Sugimori H, Nakagawa R, Takada I *et al.* Pivotal role of cerebral interleukin-17-producing gammadeltaT cells in the delayed phase of ischemic brain injury. *Nat Med* 2009; **15**: 946–950.
7. Hofstetter HH, Sewell DL, Liu F, Sandor M, Forsthuber T, Lehmann PV *et al.* Autoreactive T cells promote post-traumatic healing in the central nervous system. *J Neuroimmunol* 2003; **134**: 25–34.
8. Ziv Y, Ron N, Butovsky O, Landa G, Sudai E, Greenberg N *et al.* Immune cells contribute to the maintenance of neurogenesis and spatial learning abilities in adulthood. *Nat Neurosci* 2006; **9**: 268–275.
9. Chiu IM, Chen A, Zheng Y, Kosaras B, Tsiftsoglou SA, Vartanian TK *et al.* T lymphocytes potentiate endogenous neuroprotective inflammation in a mouse model of ALS. *Proc Natl Acad Sci USA* 2008; **105**: 17913–17918.
10. Ishii H, Jin X, Ueno M, Tanabe S, Kubo T, Serada S *et al.* Adoptive transfer of Th1-conditioned lymphocytes promotes axonal remodeling and functional recovery after spinal cord injury. *Cell Death Dis* 2012; **3**: e363.
11. Hendrix S, Nitsch R. The role of T helper cells in neuroprotection and regeneration. *J Neuroimmunol* 2007; **184**: 100–112.
12. Derecki NC, Cardani AN, Yang CH, Quinnies KM, Crihfield A, Lynch KR *et al.* Regulation of learning and memory by meningeal immunity: a key role for IL-4. *J Exp Med* 2010; **207**: 1067–1080.
13. Kebir H, Kreymborg K, Ifergan I, Dodelet-Devillers A, Cayrol R, Bernard M *et al.* Human TH17 lymphocytes promote blood-brain barrier disruption and central nervous system inflammation. *Nat Med* 2007; **13**: 1173–1175.
14. Hafler DA. Multiple sclerosis. *J Clin Invest* 2004; **113**: 788–794.
15. Fransson ME, Liljenfeldt LS, Fagius J, Tötterman TH, Loskog AS. The T-cell pool is anergized in patients with multiple sclerosis in remission. *Immunology* 2009; **126**: 92–101.
16. Hu X, Ivashkiv LB. Cross-regulation of signaling pathways by interferon-gamma: implications for immune responses and autoimmune diseases. *Immunity* 2009; **31**: 539–550.
17. Mullen AC, High FA, Hutchins AS, Lee HW, Villarino AV, Livingston DM *et al.* Role of T-bet in commitment of TH1 cells before IL-12-dependent selection. *Science* 2001; **292**: 1907–1910.
18. Basso DM, Fisher LC, Anderson AJ, Jakeman LB, McTigue DM, Popovich PG. Basso Mouse Scale for locomotion detects differences in recovery after spinal cord injury in five common mouse strains. *J Neurotrauma* 2006; **23**: 635–659.
19. Metz GA, Merkler D, Dietz V, Schwab ME, Fouad K. Efficient testing of motor function in spinal cord injured rats. *Brain Res* 2000; **883**: 165–177.
20. Ford AL, Goodsall AL, Hickey WF, Sedgwick JD. Normal adult ramified microglia separated from other central nervous system macrophages by flow cytometric sorting. Phenotypic differences defined and direct *ex vivo* antigen presentation to myelin basic protein-reactive CD4+ T cells compared. *J Immunol* 1995; **154**: 4309–4321.
21. Liesz A, Suri-Payer E, Veltkamp C, Doerr H, Sommer C, Rivest S *et al.* Regulatory T cells are key cerebroprotective immunomodulators in acute experimental stroke. *Nat Med* 2009; **15**: 192–199.
22. David S, Kroner A. Repertoire of microglial and macrophage responses after spinal cord injury. *Nat Rev Neurosci* 2011; **12**: 388–399.
23. Iannotti C, Ping Zhang Y, Shields CB, Han Y, Burke DA, Xu XM. A neuroprotective role of glial cell line-derived neurotrophic factor following moderate spinal cord contusion injury. *Exp Neurol* 2004; **189**: 317–332.
24. Ghosh A, Greenberg ME. Distinct roles for bFGF and NT-3 in the regulation of cortical neurogenesis. *Neuron* 1995; **15**: 89–103.